THE UNIVERSITY OF CHICAGO

THE TREATMENT OF DIRADICAL SYSTEMS AND MOLECULAR OPTIMIZATIONS WITH TWO-ELECTRON REDUCED DENSITY MATRICES

A DISSERTATION SUBMITTED TO
THE FACULTY OF THE DIVISION OF THE PHYSICAL SCIENCES
IN CANDIDACY FOR THE DEGREE OF
DOCTOR OF PHILOSOPHY

DEPARTMENT OF CHEMISTRY

BY
ANDREW VALENTINE

CHICAGO, ILLINOIS
AUGUST 2017

To my parents, David and Donna

TABLE OF CONTENTS

LIST OF FIGURES

LIST OF TABLES

ABSTRACT

The electronic Hamiltonian contains only pairwise interactions, allowing the energy of an electronic system to be expressed in terms of the two-electron reduced-density-matrix (2-RDM) in lieu of the many-electron wavefunction. The variable space for the exact N-electron wavefunction scales exponentially with the size of the system, while the 2-RDM is polynomial in scale. By using the 2-RDM as the primary variable in electronic structure calculations, it may be possible to obtain very accurate energies at a much more favorable scaling than wavefunction methods. In this thesis, we will use two existing 2-RDM methods to treat electronic systems. First, we will apply the active-space variational 2-RDM method, which directly minimizes the energy with respect to the 2-RDM, to a cadmium telluride polymer that was recently used to greatly enhance the conductivity of CdTe quantum dots. We find that this polymer is very highly correlated despite a deceptively simple structure. We will then turn to the parametric 2-RDM method (p2-RDM), which parameterizes the 2-RDM in terms of a truncated configuration interaction ansatz, but which includes additional flexibility in order to be size-extensive. We apply p2-RDM to the study of the olympicene molecule, which features both fully aromatic and diradical isomers. The parametric 2-RDM method predicts that all isomers are stable to dissociation, in contrast to coupled cluster methods which do not predict stable diradical states. We then present analytical nuclear gradients for p2-RDM, which greatly decrease the number of calculations required to perform geometry optimizations. We apply these gradients to the study of *trans*-polyacetylene, for which p2-RDM, unlike many wavefunction methods, is able to predict a bond length alternation (BLA) to within experimental values. Lastly, as a single-reference method, p2-RDM may encounter numerical difficulties when the reference wavefunction is of particularly poor quality. We propose a modification to the parameterization that may render the method more generally robust.

ACKNOWLEDGMENTS

This work is the product of years of effort, sometimes easy and often difficult. I am proud of what I was able to accomplish, but I acknowledge none of it would have been possible without the guidance, support, and friendship of others, to whom I would like to offer my thanks.

I would first like to thank my advisor, Professor David Mazziotti, whose insights proved invaluable throughout the years. Working in his group afforded me the opportunity to work in a very unique and promising corner of electronic structure theory. He encouraged me to aim high, and even though success seemed elusive for a very long time, he never lost faith in me. Ultimately, he taught me to trust my instincts as a researcher and to always keep trying, and these will be two of the most valuable lessons I learned during my time here.

I would also like to thank my colleagues in the Mazziotti group: Jay, Srikant, Andrew, Erik, Nick, Chad, Julie, Erica, Romit, Charles, Anthony, Manas, Ali, and Kade. They were mentors when I was first trying to find my way and friends that made everything easier along the way. Each of them had a wholly unique view of science and the work we did, which never ceased to open my eyes to new ways of thinking.

I would like to thank all of my friends at the university. They are far too many to name, but the memories we formed will be some of the longest-lasting rewards of coming here. I must of course thank the immortal Baseliners: no mercy, now or ever.

Lastly, I would like to thank my family: my brother Paul and my sister Beth, and my parents David and Donna. They were a constant source of love, encouragement, support, and advice, throughout my entire life but especially these last few years. I love them dearly.

CHAPTER 1

INTRODUCTION

1.1 Electronic Structure

Quantum mechanics, or the study of matter at very small scale, is governed by the time-dependent Schrödinger equation

$$i\hbar\frac{\partial}{\partial t}\Psi(\vec{r},t) = \hat{H}(\vec{r},t)\Psi(\vec{r},t) \tag{1.1}$$

where Ψ is the wavefunction, $\vec{r}$ is the coordinates of all the particles of the system, t is the time, and $\hat{H}$ is the Hamiltonian. This equation states that the time evolution of the system is governed by the Hamiltonian, which is given by

$$\hat{H} = \sum_{i}^{N} -\frac{\hbar^2}{2m_i}\nabla^2 + V(\vec{r},t). \tag{1.2}$$

The first term in $\hat{H}$ is the sum of the kinetic energy of each particle in the system, and $V(\vec{r},t)$ is potential energy term. If $V(\vec{r},t)$ has no explicit time-dependence, the equation in Eq. 1.1 reduces to the time-independent Schrödinger equation

$$\hat{H}\psi(\vec{r}) = E\psi(\vec{r}) \tag{1.3}$$

an eigenvalue equation whose solutions ψ_i are the possible stationary states of the system, each corresponding to an energy E_i. The wavefunction contains all the information about the system, from which we may obtain almost any property of interest. In particular, electronic structure seeks the solution to Eq. 1.3 for systems consisting of positively charged nuclei and negatively charged electrons. For these systems, if relativistic effects are neglected, the potential energy term $V_{ij} = \frac{\pm k}{|\vec{r_i}-\vec{r_j}|}$, where k is a constant whose sign is positive if the charges of the particles i and j have the same sign and negative if they have opposite

signs. Nuclei are commonly excluded from Eq. 1.3 because their mass is three orders of magnitude larger than that of electrons; from the point-of-view of the smaller, faster-moving electrons, the larger nuclei are effectively stationary. This is known as the Born-Oppenheimer approximation, reducing the search for stationary states to the solution of Eq. 1.3 with the following electronic Hamiltonian

$$\hat{H} = \sum_{i}^{N} -\frac{\hbar^2}{2m_i}\nabla^2 + \sum_{i}^{N}\sum_{I}^{M} \frac{-k}{|\vec{r_i} - \vec{R_I}|} + \sum_{i<j}^{N} \frac{k}{|\vec{r_i} - \vec{r_j}|}. \tag{1.4}$$

The first term contains the kinetic energy of the electrons, the second contains the attraction the electrons and the (frozen) nuclei, and the third term is the electron-electron repulsion.

If the system contains one electron, the Hamiltonian consists only of the first two (one-body) terms in Eq. 1.4, and the solutions ψ to Eq. 1.3 are a series of orthonormal one-particle wavefunctions, also known as orbitals. For the hydrogen atom, these form the well-known hydrogenic orbitals s, p, d, et cetera. Unfortunately, due to the two-body electron-electron repulsion term, an exact analytical solution to the electronic Schrödinger equation is impossible for more than one electron, and therefore approximate numerical solutions to this equation are required. In constructing an approximate wavefunction, one important consideration is that electrons are indistinguishable particles of half-integer spin, or fermions. The wavefunction must be antisymmetric to the exchange of two fermions, a property that can be ensured with the use of Slater determinants. An N-electron Slater determinant has the form

$$|\Phi\rangle = \frac{1}{\sqrt{N!}} \begin{vmatrix} \phi_1(1) & \phi_2(1) & \cdots & \phi_N(1) \\ \phi_1(2) & \phi_2(2) & \cdots & \phi_N(2) \\ \vdots & & \ddots & \vdots \\ \phi_1(N) & \phi_2(N) & \cdots & \phi_N(N) \end{vmatrix} \tag{1.5}$$

where ϕ_i is the ith orthonormal orbital. Exchanging two electrons has the effect of swapping two rows of the determinant, which flips the sign. No single Slater determinant constitutes

an exact solution to Eq. 1.3, but it can form a suitable basis in which to express such a solution.

A simple approximate solution to the electronic Schrödinger equation would be a single Slater determinant, with orbitals ϕ chosen so as to minimize the energy. The method for finding the orbitals ϕ is known as Hartree-Fock (HF) [1]. It begins by choosing a set of atomic orbitals (AOs), which are often Gaussian functions. The HF equations are then solved in an iterative and self-consistent fashion, producing a set of molecular orbitals (MOs) that are linear combinations of atomic orbitals (LCAOs). The N electrons are placed in the N orbitals that produce the lowest-energy determinant possible. Within the HF method, the electron-electron repulsion term in Eq. 1.4 is not treated exactly. Instead, a given electron interacts with the other $N-1$ electrons in an averaged fashion, and thus HF is known as a "mean-field" method. Despite being a simple wavefunction guess, HF frequently captures more than 99% of the total electronic energy. For this reason, many electronic structure methods use HF as a starting point in calculations; these are known as post-Hartree-Fock methods.

Once a given one-particle basis of MOs has been determined using HF, many determinants are possible other than the HF determinant $|\Phi_0\rangle$. A linear combination of all possible combinations of all N electrons placed into all r orbitals would also make a suitable wavefunction ansatz. This is the wavefunction used in full configuration interaction (full CI) [2].

$$|\psi_{FCI}\rangle = c_0|\Phi_0\rangle + \sum_{ia} c_i^a|\Phi_i^a\rangle + \sum_{\substack{i<j \\ a<b}} c_{ij}^{ab}|\Phi_{ij}^{ab}\rangle + \dots \tag{1.6}$$

where $|\Phi_{\{p\}}^{\{q\}}\rangle$ is the determinant produced by moving electrons out of the occupied orbitals $\{p\}$ into the unoccupied orbitals $\{q\}$. The energy of this wavefunction is the expectation value

$$E_{FCI} = \langle\psi_{FCI}|\hat{H}|\psi_{FCI}\rangle. \tag{1.7}$$

If the energy E_{FCI} is minimized with respect to the coefficients $\{c\}$ in Eq. 1.6, the numerically exact solution to the electronic Schrödinger equation within a given AO basis is obtained. The difference between the full CI energy and the HF energy is known as the *correlation energy*. In a real system, electrons are attracted to the nucleus but repelled by other electrons, and therefore electrons move in a correlated fashion in order to avoid one another. However, the HF wavefunction confines the N electrons into N orbitals, preventing their coordinated motion. Full CI, in contrast, does account for electron correlation by sampling among all possible electron configurations. Unfortunately, full CI scales combinatorially as ${}_rC_N$, which means that for 16 electrons and 32 spin orbitals, there are $\sim 10^9$ possible determinants. This scaling rapidly renders full CI computationally intractable, and it certainly cannot be performed for systems with more than 18 electrons and 36 spin orbitals.

Much of electronic structure is devoted to developing methods that capture as much of the correlation energy as possible, while remaining computationally inexpensive enough to treat larger molecules of chemical interest. One approximation to the exact wavefunction would be to truncate the wavefunction in Eq. 1.6 after a given excitation order, a method known as truncated CI [3]. For example, if the wavefunction were truncated at second order, the method would be configuration interaction with single and double excitations, or CISD. This approximation is reasonable because doubly excited determinants couple most strongly to the reference wavefunction, and therefore CISD should capture a large percentage of the correlation energy. Unfortunately, truncated CI methods are not size-extensive: the percentage of correlation energy they capture decreases as the system gets larger.

Size-extensive approximations to full CI are also possible, such as Møller-Plesset perturbation theory [4]. Another is coupled-cluster theory [5], which is similar to truncated CI in that it features a finite number of excitation tensors. However, it approximates higher excitations as a product of lower excitations (e.g. quadruple excitations as a product of double excitations), allowing it to to be both size extensive and substantially more accurate. The method has proved highly successful, such that coupled cluster with single and double ex-

citations with perturbative triples, CCSD(T), is often called the gold standard of electronic structure methods [6].

Active-space methods are another form of approximating full CI. In active space CI, a full CI calculation is performed within a certain number of orbitals, while the other orbitals remain either doubly occupied or empty. This method can be improved by also allowing rotations between orbitals, otherwise known as CASSCF [7]. In HF, the MOs are rotated so as to be optimal for a single determinant, whereas CASSCF rotates the MOs to be optimal for a linear combination of determinants. A CASSCF wavefunction may also be used as a reference wavefunction for multireference methods, such as MRCI, perturbation theory methods like CASPT [8] or MRMP [9], or multireference coupled cluster [10].

Another collection of electronic structure methods seek to approximate the solutions to the electronic Schrödinger equation not by using the wavefunction, but by using reduced density matrices. These will be explored in the following section.

1.2 Reduced-Density-Matrix Methods

In second quantization, the electronic Hamiltonian is expressed as

$$\hat{H} = \sum_{\substack{p<q \\ r<s}} {}^2K_{rs}^{pq} a_p^\dagger a_q^\dagger a_s a_r \tag{1.8}$$

where ${}^2K_{rs}^{pq}$ contains the one- and two-electron integrals

$${}^2K_{rs}^{pq} = \frac{1}{N-1}(\delta_{pr}\langle q|\hat{h}|s\rangle + \delta_{qs}\langle p|\hat{h}|r\rangle) + \langle pq|\hat{V}|rs\rangle. \tag{1.9}$$

and the operators $a_p^\dagger$ and a_p create and annihilate an electron in the orbital p, respectively. The creation and annihilation operators obey anticommutation relations in order to satisfy the antisymmetry requirements for fermions. The energy of a given wavefunction $|\psi\rangle$ is given

by

$$\begin{aligned} E &= \langle\psi|\hat{H}|\psi\rangle \\ &= \sum_{\substack{p<q \\ r<s}} {}^2K^{pq}_{rs}\langle\psi|a_p^\dagger a_q^\dagger a_s a_r|\psi\rangle. \end{aligned} \tag{1.10}$$

In lieu of a wavefunction, the energy can also be expressed using a reduced density matrix (RDM)

$${}^2D^{pq}_{rs} = \langle\psi|a_p^\dagger a_q^\dagger a_s a_r|\psi\rangle \tag{1.11}$$

such that Eq. 1.10 can be written as

$$E = \mathrm{Tr}({}^2K^2D). \tag{1.12}$$

Eq. 1.12 states that the energy can be exactly expressed as a function of the 2-RDM, because the Hamiltonian only contains one- and two-particle operators. The expression in Eq. 1.11 is equivalent to integrating the wavefunction over all electrons save two. The 2-RDM, therefore, only contains information about two electrons, as opposed to the N-electron wavefunction which holds information about all N. Indeed, the 2-RDM holds r^4 elements, as opposed to the exact wavefunction which contains ${}_rC_N$. The ability to exactly express the energy using an object much smaller than the N-electron wavefunction has been a tantalizing prospect for many years [11].

Unfortunately, it was noticed early on that direct minimization of the energy with respect to the elements of the 2-RDM yields energies that are far too low [12, 13]. This is because, while every N-electron wavefunction may be contracted onto a 2-RDM using Eq. 1.11, not every 2-RDM may be derived from an N-electron wavefunction. The set of all possible 2-RDMs is therefore larger than the set of all possible N-electron wavefunctions, causing energy minimizations with respect to the 2-RDM to be lower bounds to the full CI energy. This is known as the N-representability problem, and N-representability constraints are necessary to ensure the 2-RDM resembles as closely as possible a physically realistic N-

electron wavefunction [11].

The N-electron wavefunction gives the probability of finding N electrons in a given configuration. The eigenvalues of the 2-RDM, meanwhile, give the probability of finding two electrons in a given antisymmetric two-electron geminal. An important consideration for the N-representability of a 2-RDM is that the probability of that geminal being occupied must lie between 0 and 1: probabilities cannot be negative. This is equivalent to saying that the 2-RDM must be positive semidefinite

$$^2D \succeq 0 \tag{1.13}$$

or have eigenvalues greater than or equal to zero. Extending these considerations to the two-hole and one-particle-one-hole matrices Q and G

$$\begin{aligned} ^2Q^{ij}_{kl} &= \langle\psi|\hat{a}_i\hat{a}_j\hat{a}^\dagger_l\hat{a}^\dagger_k|\psi\rangle \succeq 0 \\ ^2G^{ij}_{kl} &= \langle\psi|\hat{a}^\dagger_i\hat{a}_j\hat{a}^\dagger_l\hat{a}_k|\psi\rangle \succeq 0 \end{aligned} \tag{1.14}$$

gives the DQG conditions, defined in Eqs. 1.13 and 1.14, on the variational minimization of the energy with respect to the 2-RDM [14]. While these conditions do not ensure complete N-representability, they do greatly reduce the deviation from N-representability. Energies found using these conditions remain a lower bound to the exact energy, but they are substantially more accurate than an unconstrained optimization [15, 16]. An active space formulation of the variational 2-RDM method is utilized in Chapter 2 to study a highly multireference and computationally demanding CdTe polymer.

Another way of utilizing the 2-RDM in quantum mechanical calculations is the parametric 2-RDM method (p2-RDM). In p2-RDM, partial N-representability is enforced by parameterizing the 2-RDM in terms of an N-representable wavefunction, specifically that of CISD [17]. The 2-RDM is granted additional flexibility during the optimization in order to ensure size-extensivity, but the parameterization preserves partial N-representability [17–19]. Because the majority of this thesis deals heavily with p2-RDM, its derivation is presented

more fully in Chapter 3. It is then used to examine the single-reference aromatic isomers and the diradical multireference isomers of the olympicene molecule in Chapter 4. In Chapter 5, analytical nuclear derivatives are introduced for the p2-RDM method, which greatly increase the speed of molecular optimizations. Lastly, in Chapter 6, an alteration to the parameterization is proposed to help p2-RDM treat more difficult and highly multireferenced systems.

1.3 References

[1] A. Szabo and N. S. Ostlund, *Modern Quantum Chemistry: Introduction to Advanced Electronic Structure Theory* (Dover, New York, 1996).

[2] I. Shavitt, *The Method of Configuration Interaction* (Springer US, Boston, MA, 1977), pp. 189–275.

[3] C. D. Sherrill and H. F. Schaefer III (Academic Press, 1999), vol. 34 of *Advances in Quantum Chemistry*, pp. 143 – 269.

[4] C. Møller and M. S. Plesset, Phys. Rev. **46**, 618 (1934).

[5] I. Shavitt and R. J. Bartlett, *Many-body methods in chemistry and physics: MBPT and coupled-cluster theory* (Cambridge university press, 2009).

[6] J. Rezac and P. Hobza, J. Chem. Theory Comput. **9**, 2151 (2013).

[7] B. O. Roos, P. R. Taylor, P. E. Si, et al., Chem. Phys. **48**, 157 (1980).

[8] J. Finley, P. Å. Malmqvist, B. O. Roos, and L. Serrano-Andrés, Chem. Phys. Lett. **288**, 299 (1998).

[9] K. Hirao, Chem. Phys. Lett. **190**, 374 (1992).

[10] P. Piecuch, N. Oliphant, and L. Adamowicz, J. Chem. Phys. **99**, 1875 (1993).

[11] A. J. Coleman, Rev. Mod. Phys. **35**, 668 (1963).

[12] R. H. Tredgold, Phys. Rev. **105**, 1421 (1957).

[13] A. J. Coleman and V. I. Yukalov, *Reduced density matrices: Coulsons challenge*, vol. 72 (Springer Science & Business Media, 2000).

[14] D. A. Mazziotti, Chem. Rev. **112**, 244 (2012).

[15] M. Nakata, H. Nakatsuji, M. Ehara, M. Fukuda, K. Nakata, and K. Fujisawa, J. Chem. Phys. **114**, 8282 (2001).

[16] D. A. Mazziotti, Phys. Rev. Lett. **93**, 213001 (2004).

[17] C. Kollmar, J. Chem. Phys. **125**, 084108 (2006).

[18] D. A. Mazziotti, Phys. Rev. Lett. **101**, 253002 (2008).

[19] D. A. Mazziotti, Phys. Rev. A **81**, 062515 (2010).

CHAPTER 2

ORBITALS, OCCUPATION NUMBERS, AND BAND STRUCTURE OF SHORT ONE-DIMENSIONAL CADMIUM TELLURIDE POLYMERS

This chapter contains parts of an article that was originally published in the Journal of Physical Chemistry A. Reproduced with permission from [A. J. S. Valentine, D. V. Talapin, and D. A. Mazziotti,*J. Phys. Chem. A*, **121**, 3142 (2017)].

2.1 Introduction

Semiconductor nanocrystals, or quantum dots (QDs), have electronic and spectroscopic properties currently of great interest to the research community [1]. Quantum dots, with their narrow emission spectra of tunable wavelengths, are natural building blocks for LCD displays and light-emitting devices [2]. Within the medical community, they have been used as chemiluminescent sensors [3], with applications such as immunolabeling [4] or protein detection [5, 6]. QDs have also successfully been employed as field-effect transistors (FETs) [7], and the combination of their conductive and absorption properties has rendered QDs promising candidates for next-generation solar cells [8]. More recently, a groundbreaking study by Dolzhnikov *et al.* [9] looked to increase the conductivity of a wide array of semiconductor nanocrystals. They found that by annealing QD films in the presence of soluble inorganic salts formed from the same material as the QDs (e.g. CdTe QDs in a Na_2CdTe_2 solution),

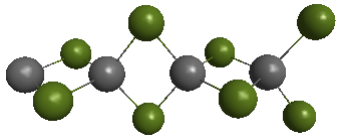

Figure 2.1: The CdTe polymer

they were able to increase dramatically the electron mobility of FETs by up to two orders of magnitude. Another study [10] found that CdTe QDs capped with Te^{2-} ligands showed markedly increased carrier mobility and diffusion length. These two studies suggest that the interface of quantum dots and inorganic materials is an important step forward in QD-based devices.

It would be useful to have a theoretical understanding of the inorganic materials that have been used to enhance QD-based FETs. To that end, this paper will examine a novel inorganic structure that was reported in the Dolzhnikov *et al.* study [9]: a $[CdTe_2^{2-}]_\infty$ polymer in a one-dimensional wire motif that had not previously been reported. This paper will offer a computational study of that polymer, reporting natural-orbital (NO) occupation numbers, Mulliken populations, charge gaps, and isomer effects as a function of polymer size and composition. As a conducting polymer, it will likely feature a high density of states near the HOMO-LUMO gap, with a correspondingly large number of nearly degenerate orbitals; as a result, the ground state of the polymer is likely highly multi-referenced. A multi-referenced wavefunction is one that cannot be qualitatively described by a single Slater determinant, and is common in systems with ground and excited states that are close in energy. Previous computational studies of small CdTe clusters have reported optimized structures and HOMO-LUMO gaps using either molecular dynamics simulations [11] or density functional theory (DFT) [12–16]. However, DFT offers a one-electron picture of electronic structure, which is inherently uncorrelated, and we expect that the polymer's nature can only be captured fully with a two-electron based method.

The variational two-electron reduced density matrix (2-RDM) method has proven to be a robust alternative to traditional wavefunction methods [17–22]. The variational 2-RDM method has been successfully applied to extended π-conjugated systems like acene sheets [23] and firefly luciferin [24], as well as to inorganic complexes such as vanadium oxo 2,6-bis[1,1-bis(2-pyridyl)ethyl]pyridine [25]. The complex in the latter paper, which featured heavy atoms and a very large number of electrons, was found to demonstrate ligand noninnocence,

but this effect could not be captured until a very large (42,40) active space was employed. The success of the 2-RDM method in handling such large active spaces renders it uniquely suited to a study of the CdTe polymer, which likewise features heavy atoms and a high number of electrons.

2.2 Theory

A common method in electronic structure is to posit a wavefunction $|\Psi\rangle$ and variationally minimize its energy

$$E = \langle\Psi|\hat{H}|\Psi\rangle \tag{2.1}$$

in order to find an upper bound to the energy of the true wavefunction. Once a wavefunction has been found, its two-electron reduced density matrix (2-RDM) may be derived by integrating over all electrons but two

$${}^2D^{ij}_{kl} = \langle\Psi|\hat{a}^\dagger_i\hat{a}^\dagger_j\hat{a}_l\hat{a}_k|\Psi\rangle \tag{2.2}$$

where $\hat{a}$ and $\hat{a}^\dagger$ are the usual annihilation and creation operators. The energy in Eq. 2.1 may then be rewritten in terms of the 2-RDM by

$$E = \mathrm{Tr}({}^2K\,{}^2D) \tag{2.3}$$

where ${}^2K$ is the reduced Hamiltonian matrix given by

$${}^2K^{ij}_{kl} = \frac{1}{N-1}(\delta_{ik}\langle j|\hat{h}|l\rangle + \delta_{jl}\langle i|\hat{h}|k\rangle) + \langle ij|\hat{V}|kl\rangle. \tag{2.4}$$

Here $\hat{h}$ and $\hat{V}$ are the one- and two-electron operators, respectively. It is possibly to minimize the energy in Eq. 2.3 directly with respect to the elements of the 2-RDM ${}^2D^{ij}_{kl}$ [26–37]. However, this results in an energy that is dramatically too low and is in fact a *lower* bound

to the energy of the true wavefunction in a given finite basis set. This is because the set of all possible 2-RDMs is much larger than the set of all possible wavefunctions; that is to say, not every 2-RDM corresponds to a physical N-electron wavefunction, or equivalently, not every 2-RDM is *N-representable* [29–33].

The constraints necessary to ensure the 2-RDM is N-representable are called p-positivity conditions [32], of which a subset are the 2-positivity conditions [38]. These state that the following matrices must have non-negative eigenvalues, or be positive-semidefinite

$$\begin{aligned} {}^2D &\succeq 0 \\ {}^2Q &\succeq 0 \\ {}^2G &\succeq 0 \end{aligned} \tag{2.5}$$

where the $\succeq$ symbol means all eigenvalues of the matrices are greater than or equal to 0. ${}^2D$, ${}^2Q$, and ${}^2G$ are the particle-particle, hole-hole, and particle-hole 2-RDMs, defined by

$$\begin{aligned} {}^2D^{ij}_{kl} &= \langle\Psi|\hat{a}^\dagger_i\hat{a}^\dagger_j\hat{a}_l\hat{a}_k|\Psi\rangle \\ {}^2Q^{ij}_{kl} &= \langle\Psi|\hat{a}_i\hat{a}_j\hat{a}^\dagger_l\hat{a}^\dagger_k|\Psi\rangle \\ {}^2G^{ij}_{kl} &= \langle\Psi|\hat{a}^\dagger_i\hat{a}_j\hat{a}^\dagger_l\hat{a}_k|\Psi\rangle. \end{aligned} \tag{2.6}$$

These constraints correspond to the physical intuition that the probabilities of finding two particles, two holes, or one particle and one hole must all be non-negative. After adding these constraints to the minimization of the energy in (3), the energy of the resulting 2-RDM remains a lower bound to the true energy, but the error is greatly decreased.

In the active-space variational 2-RDM method [39, 40], the variational minimization of the energy is performed only within a subset of the total molecular orbitals of the system, while the core orbitals remain doubly occupied, in a fashion analogous to complete active space configuration interaction (CASCI). To further improve the accuracy of the solution, we can also minimize the energy of the 2-RDM with respect to the molecular orbitals them-

selves, rendering the method effectively analogous to complete active-space self-consistent field (CASSCF) [41]. In practice, the algorithm proceeds by minimizing the energy as a function of the 2-RDM within the active space, mixing the active and inactive orbitals by one-electron unitary transformations to lower the energy further, and repeating until the energy of the 2-RDM converges.

2.3 Applications

The active-space variational 2-RDM method is used to investigate the $[CdTe_2^{2-}]_n$ polymer. Occupation numbers, natural orbitals, and band gaps are reported for n from 1 to 4. For the largest polymer, occupation numbers and Mulliken charges are presented for its oxidized and reduced states. Occupation numbers are also given for other, more symmetric forms of the polymer, capped with either a Cd^{2+} or Te_2^{4-} unit.

2.3.1 Methodology

All calculations were performed in the 3-21G split valence basis set [42]. The active-space variational two-electron reduced density matrix method was used to calculate ground-state energies and natural-orbital occupation numbers of various forms of the $[CdTe_2^{2-}]_n$ polymer. The active space consisted of the $5sp$ orbitals for each Cd and Te atom, with the sole exception of the tetramer calculations, which excluded the $5s$ orbitals of Te due to excessive computational costs. All core orbitals were taken to be frozen; that is, the orbital rotation mentioned above was not performed for any of the doubly occupied orbitals. Generation of the molecular orbitals from Hartree-Fock calculations as well as evaluation of one- and two-electron integrals were performed using the GAMESS electronic structure package [43]. The oxidized and reduced forms of the polymer, which are doublets, were treated by calculating the ground state of the molecule together with a single hydrogen atom placed at infinite separation [21]. In all calculations, Cd was taken to be in a 2+ oxidation state and Te in a

2− oxidation state for the purpose of electron counts. Bond lengths and bond angles of the polymer were taken from Ref. [9]. The polymer used in Ref. [9] as a conducting filler between quantum dots was anionic, with a −2 charge per monomer unit. This charge allowed the polymer to be dissolved in solution, but the additional electrostatic repulsion from the extra electrons renders the polymer highly unstable in the gas phase; for that reason, total energies of the molecule are not reported here.

2.3.2 Results

The molecular orbital (MO) diagram for the $CdTe_2^{2-}$ monomer, obtained from Hartree-Fock in the 3-21G basis, is plotted in Fig. 2.2. It is readily apparent that the occupied $4d$-shell orbitals on the cadmium are much lower in energy than the other valence orbitals. In practice, when these orbitals are included in the active space, they contribute minimally to the electronic structure and largely remain doubly occupied. This is consistent with other results in the literature, and it has been argued [44] that although d^{10} group elements are found in the d-block of the periodic table, due to their completely filled d-shell, they do not behave as transition metals. The primary valence shell in $CdTe_2^{2-}$ consists of the $5s$ and $5p$ orbitals on both the cadmium and tellurium atoms, which is the active space employed in nearly all of the calculations. The $5s$ orbitals on Te are also very low in energy and mix minimally with the remainder of the active space; these orbitals are excluded from the active space in the case of the largest polymer studied, the tetramer. The next set of unoccupied MOs, arising from the $6s$ and $6p$ orbitals on the cadmium atom, do not qualitatively change the electronic structure when included in the active space. It is interesting to note that even this relatively modest (12o,16e) active space per monomer unit is computationally unfeasible for analogous MCSCF methods for the dimer, and CASSCF would require $\sim 10^{24}$ determinants in order to treat the tetramer in this active space.

Natural-orbital (NO) occupation numbers of the polymer for lengths from $n = 1$ to $n = 4$ may be found in Table 2.1. Relatively little multireference electron correlation was found

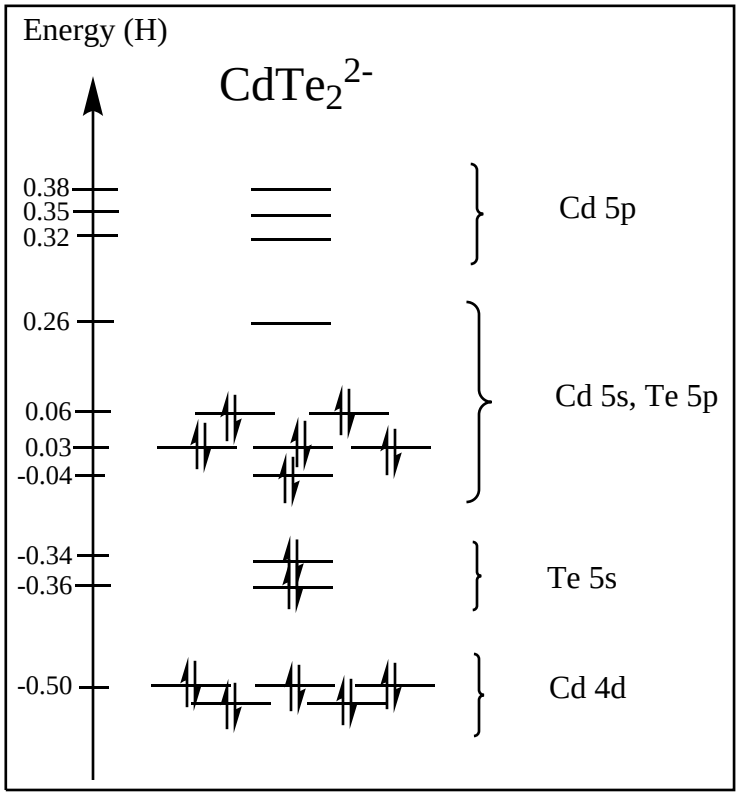

Figure 2.2: Qualitative molecular orbital diagram for the $CdTe_2^{2-}$ monomer, obtained from Hartree-Fock in a 3-21G basis set. The primary valence shell is composed of $5s$ and $5p$ orbitals from both Cd and Te.

Table 2.1: Natural-orbital occupation numbers for the $[CdTe2_2^{2-}]_n$ polymer for n from 1 to 4. In a perfectly uncorrelated molecule, the occupation of all orbitals up to the HONO would be 1 and all other orbitals would be zero. Multireference correlation increases as the polymer lengthens.

Orbital	1-mer	2-mer	3-mer	4-mer
HONO-2	0.9776	0.9610	0.9180	0.8869
HONO-1	0.9544	0.9588	0.9125	0.8131
HONO	0.9505	0.6148	0.6861	0.8042
LUNO	0.1070	0.5402	0.6795	0.7665
LUNO+1	0.0208	0.0237	0.0288	0.0291
LUNO+2	0.0202	0.0231	0.0278	0.0255

in the $CdTe_2^{2-}$ monomer, as measured by the population of the lowest-unoccupied natural orbital (LUNO) and above. In contrast, once the $Cd_2Te_4^{4-}$ dimer has been formed, we see an almost even population of the highest-occupied natural orbital (HONO) and the LUNO, with the dimer being a near diradical. Further increasing the size of the polymer to the trimer and tetramer continues to fill the HONO and LUNO evenly. Once the size of the tetramer is reached, we see remarkably even filling of the HONO, LUNO, and several other more-occupied orbitals, while the LUNO+1 and lower-occupied orbitals continue to remain energetically unfavorable. This fairly unusual filling pattern is indicative of very strong multireference correlation effects.

Select NOs from Table 2.1 are plotted in Fig. 2.3. The HONO and LUNO for both the monomer and dimer are qualitatively similar, with one orbital on each end of the molecule. However, while the populations of the HONO and LUNO are very different on the monomer, the spatial separation of these orbitals in the dimer allows them to become energetically competitive and hence, relatively equally filled. As the molecule expands to the trimer, the frontier orbitals located at either end of the molecule continue to fill, while two additional occupied NOs begin to have significant deviations in their populations from 1. Finally, in the tetramer we observe even more orbitals becoming significantly correlated. However, unlike the smaller molecules, the terminating NOs have now filled to the point where the majority of the active electron correlation is occurring in the interior of the polymer, with four frontier

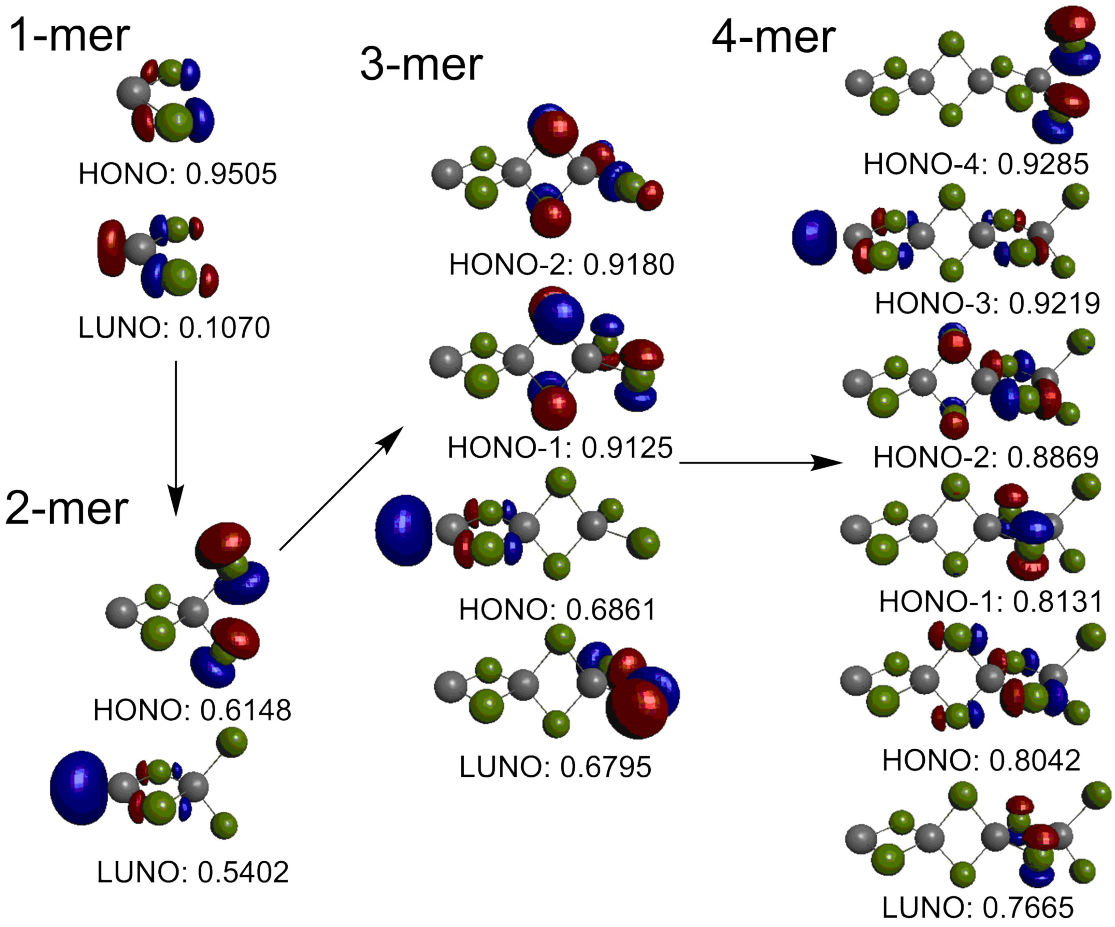

Figure 2.3: The density contours of natural orbitals are plotted for each n-mer with n from 1 to 4, where the arrow is in the direction of polymer growth. More orbitals have occupations differing substantially from 1 or 0 as the polymer grows in length.

NOs centered on the internal tellurium atoms. It may be observed that the tetramer is the first instance of a completely internal $Cd_2Te_4^{4-}$ unit, and therefore might be the first case which qualitatively represents the formation of a polymer. In such a polymer, we would expect the internal structure to dominate the edge effects of the molecule, which is what we begin to observe here.

To explore further the electron correlation of the CdTe polymer, we analyze calculations in which the polymer is either oxidized or reduced by one electron. Additionally, because different forms of the polymer could be found in solution depending on how it is cleft, isomers of the polymer were examined that were capped with either Cd^{2+} or Te_2^{4-}. The NO

occupation numbers for these two cases are presented in Fig. 2.4 for the longest molecule studied. In Fig. 2.4(a), it may be seen that adding an extra electron uniformly increased the population of the occupied orbitals and the LUNO, effectively decreasing the correlation in the system, while removing an electron substantially lowered the populations of a large number of occupied orbitals, greatly increasing the degree of multireference correlation. As with all of the examples in Table 2.1, the populations of the LUNO+1 orbital and above remain negligible regardless of electron number. Similarly, in Fig. 2.4(b), capping the polymer with Te_2^{4-} dramatically quenched the static correlation in the system, yielding a molecule that is almost entirely single-reference. In contrast, capping with Cd^{2+} greatly increased the static correlation, with substantial electron populations of both the LUNO and LUNO+1 orbitals, while LUNO+2 and above remain unfilled. The striking similarity between these two plots may be explained by the nature of the two caps. Te_2^{4-} contributes 8 completely filled orbitals to the active space, thereby increasing the relative electron filling of the system, while Cd^{2+} contributes 4 unfilled orbitals to the active space, decreasing the relative filling. The fact that the LUNO+1 (or LUNO+2 in the case of the cadmium-capped molecule) orbital and less-filled orbitals *never* receive any substantial filling strongly suggests the formation of a *band structure*, where the orbitals of the conduction band are substantially higher in energy than those of the valence band. This suggests that the polymer is a semiconductor whose valence band is nearly, but not fully filled. The *fundamental charge gap*, defined as the difference between the ionization energy and the electron affinity, was also evaluated for each species. This quantity steadily decreases with polymer length from 100.3 kcal/mol in the monomer to 78.3 in the dimer, 67.4 in the trimer, and lastly to 55.9 in the tetramer. This decreasing charge gap suggests that the polymer becomes an increasingly good conductor as it grows in length. Finally, Mulliken populations for the three oxidation states of the tetramer are plotted in Fig. 2.5, showing the distribution of the additional anionic charge across the molecule. In all three cases, the internal cadmium atoms remain largely neutral, with the additional electrons distributed across the terminating atoms and the internal tel-

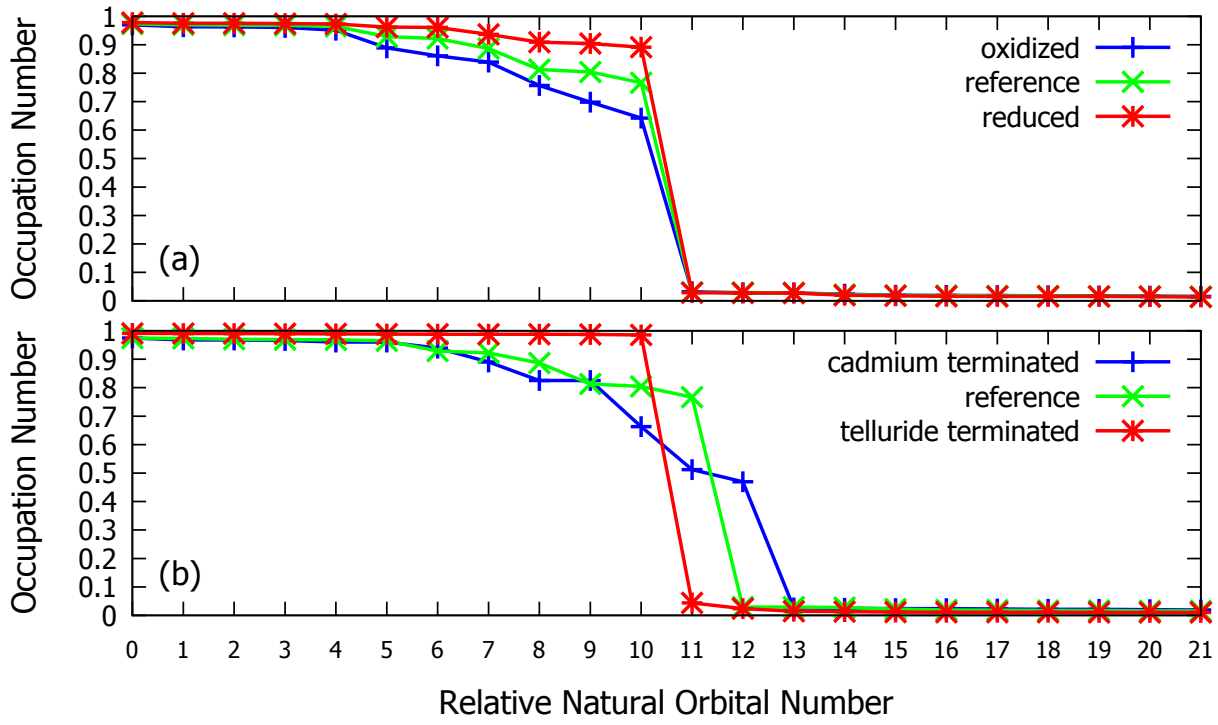

Figure 2.4: Natural-orbital occupation numbers near the HONO-LUNO gap in the $Cd_4Te_8^{8-}$ tetramer for (a) its oxidized, reference, and reduced states, and (b) the polymer capped with Cd^{2+}, the reference polymer, and the polymer capped with Te_2^{4-}. Increasing the number of electrons decreases the static correlation in the molecule, while decreasing the number of electrons increases it. Similarly, capping the polymer with the electron-rich Te_2^{4-} group decreases the static correlation, and capping with the electron-deficient Cd^{2+} cation greatly increases it.

lurium atoms; the electron added or removed from the system is largely delocalized over these atoms.

2.4 Discussion and Conclusion

In this paper, we presented the first computational study of the newly synthesized one-dimensional CdTe polymer. Natural-orbital occupation numbers show that the polymer is strongly correlated, and that its strong electron correlation increases as the polymer grows in size. However, this static correlation presents itself in an unusual fashion, with nearly even electron fillings of several of the HONOs and the LUNO, while the LUNO+1 and less-filled

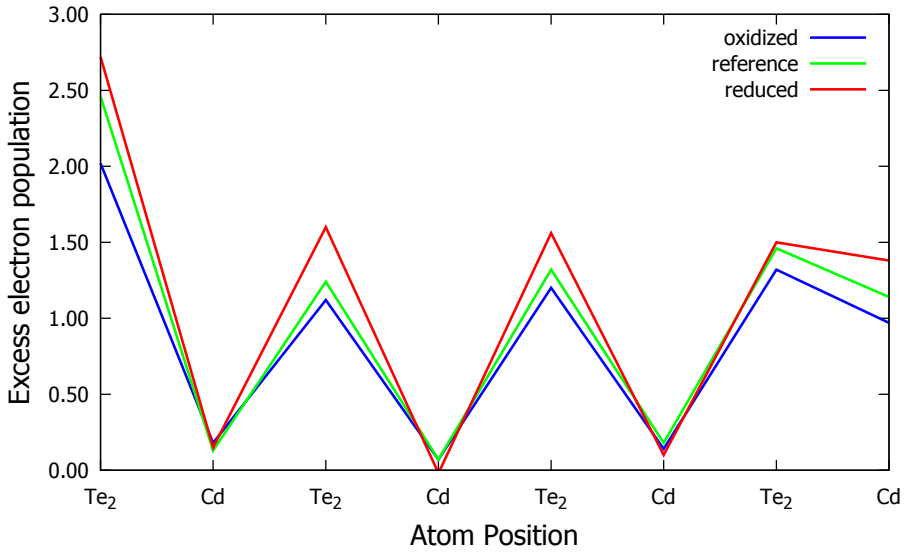

Figure 2.5: Mulliken charges of the $Cd_4Te_8^{8-}$ tetramer. The locations of the -7 charge of the oxidized species, the -8 charge of the reference species, and the -9 charge of the reduced species are plotted by atom in the polymer. The Mulliken charges have been multiplied by -1 for aesthetic reasons. Anionic charge accumulates on the ends of the molecule and on the internal Te atoms.

orbitals remain unoccupied even in the longest polymer. This suggests that there are several degenerate orbitals grouped together near the HONO-LUNO gap, forming a band, while the other LUNOs remain significantly higher in energy and are therefore inaccessible to the ground state. This is further supported by changing the number of electrons: reducing the polymer does not half-fill an unoccupied orbital, but rather fills the grouped orbitals nearly evenly, while oxidizing the polymer evenly decreases their occupation. In similar fashion, capping the polymer with an additional atom or atoms increases the number of orbitals above and below the HONO-LUNO gap, but the electron-rich Te_2^{4-} group yields a valence band that is relatively more filled, while the electron-deficient Cd^{2+} cap gives a valence band that is relatively less filled. Taking these results together, it seems very likely that the CdTe polymer possesses an almost (but not completely) filled valence band and an unfilled conduction band. Relatedly, the fundamental charge gap, defined as the difference between the ionization energy and electron affinity, decreases with polymer length, suggesting that it becomes an increasingly good conductor.

The relative electron filling of the polymer will assuredly impact its solubility and reactivity, and as this study has shown, it will also greatly impact the electronic structure of the molecule and the degree of strong electron correlation it contains. Consequently, it seems possible, by oxidation, reduction, or doping, to tune any potential QD fillers to have the ideal balance of chemical and electronic properties in order to boost maximally the conductivity of QD films. Good QD fillers will also likely be strongly correlated materials, in order to maximize the density of states near the HOMO-LUMO gap and facilitate the free flow of electrons through the molecule. The interaction of QDs and inorganic materials is an exciting new development in the field of inorganic chemistry, with the promise of yielding new QD-based devices, such as next-generation solar cells, with ever greater power and efficiency.

2.5 References

[1] M. Amelia, C. Lincheneau, S. Silvi, and A. Credi, Chem. Soc. Rev. **41**, 5728 (2012).

[2] G. J. Supran, Y. Shirasaki, K. W. Song, J.-M. Caruge, P. T. Kazlas, S. Coe-Sullivan, T. L. Andrew, M. G. Bawendi, and V. Bulović, MRS Bulletin **38**, 703 (2013).

[3] J. F. Callan, A. P. De Silva, R. C. Mulrooney, and B. Mc Caughan, J. Incl. Phenom. Macrocycl. Chem. **58**, 257 (2007).

[4] A. P. Alivisatos, W. Gu, and C. Larabell, Annu. Rev. Biomed. Eng. **7**, 55 (2005).

[5] D. Du, J. Ding, Y. Tao, H. Li, and X. Chen, Biosens. Bioelectron. **24**, 863 (2008).

[6] K. Pinwattana, J. Wang, C.-T. Lin, H. Wu, D. Du, Y. Lin, and O. Chailapakul, Biosens. Bioelectron. **26**, 1109 (2010).

[7] D. V. Talapin, J.-S. Lee, M. V. Kovalenko, and E. V. Shevchenko, Chem. Rev. **110**, 389 (2010).

[8] P. V. Kamat, J. Phys. Chem. C **112**, 18737 (2008).

[9] D. S. Dolzhnikov, H. Zhang, J. Jang, J. S. Son, M. G. Panthani, T. Shibata, S. Chattopadhyay, and D. V. Talapin, Science **347**, 425 (2015).

[10] R. W. Crisp, R. Callahan, O. G. Reid, D. S. Dolzhnikov, D. V. Talapin, G. Rumbles, J. M. Luther, and N. Kopidakis, J. Phys. Chem. Lett. **6**, 4815 (2015).

[11] J. Wang, L. Ma, J. Zhao, and K. A. Jackson, J. Chem. Phys. **130**, 214307 (2009).

[12] S. K. Bhattacharya and A. Kshirsagar, Phys. Rev. B **75**, 035402 (2007).

[13] Z. Wu, Y. Zhang, S. Huang, and S. Zhang, Comput. Mater. Sci. **68**, 238 (2013).

[14] P. Seal, S. Sen, and S. Chakrabarti, Chem. Phys. **367**, 152 (2010).

[15] A. E. Kuznetsov, D. Balamurugan, S. S. Skourtis, and D. N. Beratan, J. Phys. Chem. C **116**, 6817 (2012).

[16] E. Lim, A. E. Kuznetsov, and D. N. Beratan, Chem. Phys. **407**, 97 (2012).

[17] R. Erdahl and B. Jin, *On Calculating Approximate and Exact Density Matrices* (Springer US, Boston, MA, 2000), pp. 57–84.

[18] D. A. Mazziotti, Phys. Rev. Lett. **106**, 083001 (2011).

[19] D. A. Mazziotti, Chem. Rev. **112**, 244 (2012).

[20] A. E. Rothman and D. A. Mazziotti, Phys. Rev. A **78**, 032510 (2008).

[21] J. R. Hammond and D. A. Mazziotti, Phys. Rev. A **73**, 062505 (2006).

[22] N. C. Rubin and D. A. Mazziotti, J. Phys. Chem. C **119**, 14706 (2015).

[23] K. Pelzer, L. Greenman, G. Gidofalvi, and D. A. Mazziotti, J. Phys. Chem. A **115**, 5632 (2011).

[24] L. Greenman and D. A. Mazziotti, J. Chem. Phys. **133**, 164110 (2010).

[25] A. W. Schlimgen, C. W. Heaps, and D. A. Mazziotti, J. Phys. Chem. Lett. **7**, 627 (2016).

[26] D. A. Mazziotti, ed., *Reduced-Density-Matrix Mechanics: With Application to Many-electron Atoms and Molecules*, vol. 134 of *Adv. Chem. Phys.* (Wiley, New York, 2007).

[27] M. Mihailovl and M. Rosina, Nucl. Phys. A **237**, 229 (1975).

[28] C. Garrod, M. V. Mihailovi, and M. Rosina, J. Math. Phys. **16**, 868 (1975).

[29] R. Erdahl, Rep. Math. Phys. **15**, 147 (1979).

[30] M. Nakata, H. Nakatsuji, M. Ehara, M. Fukuda, K. Nakata, and K. Fujisawa, J. Chem. Phys. **114**, 8282 (2001).

[31] Z. Zhao, B. J. Braams, M. Fukuda, M. L. Overton, and J. K. Percus, J. Chem. Phys. **120**, 2095 (2004).

[32] D. A. Mazziotti and R. M. Erdahl, Phys. Rev. A **63**, 042113 (2001).

[33] D. A. Mazziotti, Phys. Rev. Lett. **93**, 213001 (2004).

[34] G. Gidofalvi and D. A. Mazziotti, J. Chem. Phys. **126**, 024105 (2007).

[35] B. Verstichel, H. van Aggelen, D. Van Neck, P. W. Ayers, and P. Bultinck, Phys. Rev. A **80**, 032508 (2009).

[36] H. van Aggelen, B. Verstichel, P. Bultinck, D. Van Neck, P. W. Ayers, and D. L. Cooper, J. Chem. Phys. **132**, 114112 (2010).

[37] B. Verstichel, H. van Aggelen, D. Van Neck, P. W. Ayers, and P. Bultinck, J. Chem. Phys. **132**, 114113 (2010).

[38] C. Garrod and J. K. Percus, J. Math. Phys. **5**, 1756 (1964).

[39] G. Gidofalvi and D. A. Mazziotti, J. Chem. Phys. **129**, 134108 (2008).

[40] L. Greenman and D. A. Mazziotti, J. Chem. Phys. **130**, 184101 (2009).

[41] B. O. Roos, P. R. Taylor, and P. E. Sigbahn, Chem. Phys. **48**, 157 (1980).

[42] J. S. Binkley, J. A. Pople, and W. J. Hehre, J. Am. Chem. Soc. **102**, 939 (1980).

[43] M. W. Schmidt, K. K. Baldridge, J. A. Boatz, S. T. Elbert, M. S. Gordon, J. H. Jensen, S. Koseki, N. Matsunaga, K. A. Nguyen, S. Su, et al., J. Comput. Chem. **14**, 1347 (1993).

[44] W. B. Jensen, J. Chem. Educ. **80**, 952 (2003).

CHAPTER 3

THE PARAMETRIC TWO-ELECTRON REDUCED-DENSITY-MATRIX METHOD

3.1 Introduction

In Chapter 1, it was observed that the energy of a system may be expressed using the two-electron reduced-density matrix (2-RDM).

$$E = \mathrm{Tr}({}^2K\,{}^2D) \tag{3.1}$$

where ${}^2K$ is the reduced Hamiltonian matrix and ${}^2D$ is the 2-RDM, which may be obtained from the N-electron wavefunction $|\Psi\rangle$ by

$${}^2D^{pq}_{rs} = \langle\Psi|a^\dagger_p a^\dagger_q a_s a_r|\Psi\rangle. \tag{3.2}$$

Here $a^\dagger$ and a are creation and annihilation operators, respectively. It would be advantageous to be able to evaluate the 2-RDM directly without first requiring the full N-electron wavefunction. However, it is difficult to directly determine the 2-RDM while also constraining it to correspond to a physically realistic N-electron wavefunction, which is known as an N-representable 2-RDM [1–3]. One approach is to directly minimize the energy in Eq. 3.1 while constraining the eigenvalues of various RDMs to be non-negative, which are known as p-positivity conditions [4–9]. A very different approach is to enforce N-representability by directly parameterizing the 2-RDM in terms of an N-electron wavefunction, such as the wavefunction from a truncated configuration interaction method. The derivation of such a method is the subject of this chapter.

3.2 From Configuration Interaction to a 2-RDM

The wavefunction ansatz for configuration interaction with double excitations (CID) [10, 11] is given by

$$|\Psi_{CID}\rangle = T_0|\Phi_0\rangle + \sum_{\substack{i<j \\ a<b}} {}^2T_{ij}^{ab}|\Phi_{ij}^{ab}\rangle \tag{3.3}$$

where $|\Phi_{ij}^{ab}\rangle$ is the Slater determinant formed by exciting two electrons out of the occupied orbitals i and j into the orbitals a and b. Orbitals that are occupied in the reference wavefunction are denoted by the letters (i, j, k, l), unoccupied orbitals are denoted by (a, b, c, d), and generic orbitals are given the letters (p, q, r, s). The wavefunction is normalized, such that

$$T_0 = \sqrt{1 - \sum_{\substack{i<j \\ a<b}} ({}^2T_{ij}^{ab})^2}. \tag{3.4}$$

When the energy $E = \langle\Psi|H|\Psi\rangle$ is minimized with respect to the coefficients ${}^2T$, the CID energy is obtained.

It is possible to directly contract the wavefunction in Eq. 3.3 onto a 2-RDM using the relation in Eq. 3.2. To illustrate how this occurs, consider the case where (p, q, r, s) in Eq. 3.2 are equal to (a, b, c, d), i.e. all four orbitals are unoccupied in the reference. This is the ${}^2D_{cd}^{ab}$ element of the 2-RDM, given by

$${}^2D_{cd}^{ab} = \langle\Psi_{CID}|a_a^\dagger a_b^\dagger a_d a_c|\Psi_{CID}\rangle. \tag{3.5}$$

This expectation value can only be non-zero for terms on the left where the orbitals a and b are occupied, and terms on the right where the orbitals c and d are occupied. This means that only excited determinants contribute to this term. In addition, the holes i and j in terms on the left must match up with holes k and l in terms on the right. As a result, this

element of the 2-RDM can be expressed in terms of ${}^2T$ amplitudes by

$$ {}^2D^{ab}_{cd} = \sum_{i<j} {}^2T^{ab}_{ij} {}^2T^{cd}_{ij}. \tag{3.6} $$

There are various classes of terms within ${}^2D^{pq}_{rs}$, depending on the number of orbitals that are occupied or virtual within the reference. The remainder of this chapter will closely follow the presentation of parametric 2-RDM methods given in Ref. [12]. The complete list of all terms are as follows

$$ {}^2D^{ij}_{kl} = 4{}^2I^{ij}_{kl} + 4({}^1\Delta^i_k \wedge {}^1I^j_l) + {}^2\Delta^{ij}_{kl} \tag{3.7} $$

$$ {}^2D^{ia}_{jb} = {}^1I^i_j {}^1\Delta^a_b + {}^2\Delta^{ia}_{jb} \tag{3.8} $$

$$ {}^2D^{ab}_{cd} = {}^2\Delta^{ab}_{cd} \tag{3.9} $$

$$ {}^2D^{ab}_{ij} = {}^2\Delta^{ab}_{ij} \tag{3.10} $$

where ${}^1I^p_q$ is the one-particle identity matrix, ${}^2I^{pq}_{rs}$ is the two-particle identity matrix expressed as a Grassman wedge product of one-particle matrices

$$ \begin{aligned} {}^2I^{pq}_{rs} &= {}^1I^p_r \wedge {}^1I^q_s \\ &= {}^1I^{p1}_r I^q_s - {}^1I^{p1}_s I^q_r \end{aligned} \tag{3.11} $$

and the assorted ${}^1\Delta^p_q$ and ${}^2\Delta^{pq}_{rs}$ terms are given in terms of ${}^2T$

$$ {}^2\Delta^{ij}_{kl} = \sum_{a<b} {}^2T^{ab}_{ij} {}^2T^{ab}_{kl} \tag{3.12} $$

$$ {}^2\Delta^{ia}_{jb} = -\sum_{kc} {}^2T^{ac}_{jk} {}^2T^{bc}_{ik} \tag{3.13} $$

$$ {}^2\Delta^{ab}_{cd} = \sum_{i<j} {}^2T^{ab}_{ij} {}^2T^{cd}_{ij}. \tag{3.14} $$

$$ {}^1\Delta^i_j = -\sum_{a<b}\sum_k {}^2T^{ab}_{ik}{}^2T^{ab}_{jk} \tag{3.15} $$

$$ {}^1\Delta^a_b = \sum_{i<j}\sum_c {}^2T^{ac}_{ij}{}^2T^{bc}_{ij}. \tag{3.16} $$

The final ${}^2\Delta$ term is the only one featuring the coefficient of the reference

$$ \begin{aligned} {}^2\Delta^{ab}_{ij} &= {}^2T^{ab}_{ij}T_0 \\ &= {}^2T^{ab}_{ij}\sqrt{1-\sum_{\substack{k<l\\c<d}}({}^2T^{cd}_{kl})^2}. \end{aligned} \tag{3.17} $$

Now that the 2-RDM has been parameterized in this fashion, direct minimization of the energy $E = \mathrm{Tr}({}^2K{}^2D)$ with respect to the coefficients ${}^2T$ will also yield the CID ground state energy. In this instance, the 2-RDM is exactly N-representable because it was contracted directly from the N-electron wavefunction in Eq. 3.3. However, the energies obtained from CID suffer from a lack of size-extensivity, which the following section will attempt to address.

3.3 Size-Extensivity of the Parametric 2-RDM Method

The CID parameterization in the previous chapter is not size-extensive [13]. A size-extensive method gives a correlation energy that scales linearly with the size of the system, but the expression for ${}^2\Delta^{ab}_{ij}$ used in Eq. 3.17 does not do so. Whenever $\{i,j\}\cap\{k,l\} = \emptyset$ and $\{a,b\}\cap\{c,d\} = \emptyset$, ${}^2\Delta^{ab}_{ij}$ contains unconnected terms which scale quadratically with system size. The parameterization could be rendered size-extensive by the insertion of a topological factor f into Eq. 3.17

$$ {}^2\Delta^{ab}_{ij} = {}^2T^{ab}_{ij}\sqrt{1-\sum_{\substack{k<l\\c<d}} f^{abcd}_{ijkl}({}^2T^{cd}_{kl})^2} \tag{3.18} $$

with the requirement that $f^{abcd}_{ijkl} = 0$ whenever $\{i,j,a,b\}\cap\{k,l,c,d\} = \emptyset$. This is known as the parametric 2-RDM method (p2-RDM) [12, 14, 15]. If f were equal to 1 in all cases, this method would be exactly equivalent to CID, which would be N-representable but not

size-extensive. If f were set to 0 in call cases, it would be equivalent to CEPA(0) [16–18], which is size-extensive but deviates greatly from N-representability. There may be a parameterization somewhere between two methods that is approximately N-representable and also approximately size-extensive.

Kollmar [14] noted that the 2-positivity conditions DQG could be imposed in order to enforce approximate N-representability. These state that the following matrices must all have non-negative eigenvalues

$$\begin{aligned} {}^2D &\succeq 0 \\ {}^2Q &\succeq 0 \\ {}^2G &\succeq 0 \end{aligned} \tag{3.19}$$

where ${}^2D$, ${}^2Q$, and ${}^2G$ are the two-particle, two-hole, and one-particle-one-hole RDMs, respectively

$$\begin{aligned} {}^2D^{pq}_{rs} &= \langle\Psi|a_p^\dagger a_q^\dagger a_s a_r|\Psi\rangle \\ {}^2Q^{pq}_{rs} &= \langle\Psi|a_p a_q a_s^\dagger a_r^\dagger|\Psi\rangle \\ {}^2G^{pq}_{rs} &= \langle\Psi|a_p^\dagger a_q a_s^\dagger a_r|\Psi\rangle. \end{aligned} \tag{3.20}$$

The ${}^2Q$ and ${}^2G$ matrices can be directly expressed in terms of ${}^2D$, such that the DQG conditions can be fullfilled solely by imposing constraints on ${}^2D$. Rather than directly impose DQG conditions on the optimization of the energy, the topological factor f could be chosen so as to partially fulfill the conditions implicitly. The 2-positivity conditions imply a weaker set of restrictions known as Cauchy-Schwarz inequalities, given as

$$\begin{aligned} ({}^2D^{ab}_{ij})^2 &\leq {}^2D^{ij}_{ij}\,{}^2D^{ab}_{ab} \\ ({}^2Q^{ab}_{ij})^2 &\leq {}^2Q^{ij}_{ij}\,{}^2Q^{ab}_{ab} \end{aligned} \tag{3.21}$$

for ${}^2D$ and ${}^2Q$, respectively. For ${}^2G$, there are four inequalities

$$\begin{aligned}
({}^2G^{jb}_{ia})^2 &\leq {}^2G^{ia}_{ia}{}^2G^{jb}_{jb} \\
({}^2G^{aj}_{ib})^2 &\leq {}^2G^{ib}_{ib}{}^2G^{aj}_{aj} \\
({}^2G^{bi}_{ja})^2 &\leq {}^2G^{ja}_{ja}{}^2G^{bi}_{bi} \\
({}^2G^{ai}_{jb})^2 &\leq {}^2G^{jb}_{jb}{}^2G^{ai}_{ai}.
\end{aligned} \tag{3.22}$$

The Cauchy-Schwarz are necessary conditions for any matrix to be positive semidefinite, and are sufficient in the special case of $2x2$ matrices. Substituting the expressions from Equations 3.7-3.10 into the inequalities in Eq. 3.21 and equating the connected portions give the following parameterizations

$${}^2\Delta^{ab}_{ij} = {}^2T^{ab}_{ij}(1 + {}^1\Delta^i_i + {}^1\Delta^j_j + {}^2\Delta^{ij}_{ij})^{1/2} \tag{3.23}$$

$${}^2\Delta^{ab}_{ij} = {}^2T^{ab}_{ij}(1 - {}^1\Delta^a_a + {}^1\Delta^b_b + {}^2\Delta^{ab}_{ab})^{1/2} \tag{3.24}$$

which are known as the D and Q functionals [12], respectively. Repeating the same process for the ${}^2G$ inequalities gives

$$\begin{aligned}
{}^2\Delta^{ab}_{ij} &= {}^2T^{ab}_{ij}(1 + {}^1\Delta^j_j - {}^1\Delta^b_b - {}^2\Delta^{jb}_{jb})^{1/2} \\
{}^2\Delta^{ab}_{ij} &= {}^2T^{ab}_{ij}(1 + {}^1\Delta^j_j - {}^1\Delta^a_a - {}^2\Delta^{ja}_{ja})^{1/2} \\
{}^2\Delta^{ab}_{ij} &= {}^2T^{ab}_{ij}(1 + {}^1\Delta^i_i - {}^1\Delta^b_b - {}^2\Delta^{ib}_{ib})^{1/2} \\
{}^2\Delta^{ab}_{ij} &= {}^2T^{ab}_{ij}(1 + {}^1\Delta^i_i - {}^1\Delta^a_a - {}^2\Delta^{ia}_{ia})^{1/2}.
\end{aligned} \tag{3.25}$$

Kollmar averaged the four ${}^2G$ equalities in order to derive a functional known as the K functional [14]. Mazziotti, meanwhile, chose to use the ${}^2D$ and ${}^2Q$ equalities to derive a functional that preserved particle-hole symmetry, known as the M functional [12]. Each of the functionals discussed here may be characterized by the value of f^{abcd}_{ijkl} for the number of orbitals n_o shared between (i, j) and (k, l), and the number of orbitals n_v shared between

Table 3.1: Various functionals f^{abcd}_{ijkl}, defined for classes of n_o/n_v, where n_o is the number of orbitals shared between (i,j) and (k,l), and n_v is the number shared between (a,b) and (c,d).

	Topological factor f^{abcd}_{ijkl}								
Method	0/0	1/0	2/0	0/1	0/2	1/1	2/1	1/2	2/2
CID	1	1	1	1	1	1	1	1	1
CEPA(0)	0	0	0	0	0	0	0	0	0
D	0	1	1	0	0	1	1	1	1
Q	0	0	0	1	1	1	1	1	1
K	0	1/2	1	1/2	1	3/4	1	1	1
M	0	0	1	0	1	1	1	1	1

(a,b) and (c,d). The functionals are given in terms of n_o and n_v in Table 3.1.

3.4 Incorporating Single Excitations

Regardless of functional, the parametric 2-RDM method may be improved by adding single excitations to the parameterization. Where before we started with the wavefunction from CID, we now begin with a wavefunction from configuration interaction with single and double excitations, or CISD

$$|\Psi_{CISD}\rangle = T_0|\Phi_0\rangle + \sum_{ia} {}^1T^a_i|\Phi^a_i\rangle + \sum_{\substack{i<j\\a<b}} {}^2T^{ab}_{ij}|\Phi^{ab}_{ij}\rangle. \tag{3.26}$$

The same procedure for contracting this wavefunction onto a 2-RDM is performed, as before, giving the following terms for the 2-RDM

$${}^2D^{ij}_{kl} = 4{}^2I^{ij}_{kl} + 4({}^1\Delta^i_k \wedge {}^1I^j_l) + {}^2\Delta^{ij}_{kl} \tag{3.27}$$

$${}^2D^{ia}_{jb} = {}^1I^{i\,1}_j\Delta^a_b - {}^1T^{b1}_i T^a_j + {}^2\Delta^{ia}_{jb} \tag{3.28}$$

$${}^2D^{ia}_{jk} = {}^1I^{i\,1}_j\Delta^a_k - {}^1I^{i\,1}_k\Delta^a_j + {}^2\Delta^{ia}_{jk} \tag{3.29}$$

$${}^2D^{ia}_{bc} = {}^2\Delta^{ia}_{bc} \tag{3.30}$$

$$ {}^2D^{ab}_{cd} = {}^2\Delta^{ab}_{cd} \tag{3.31} $$

$$ {}^2D^{ab}_{ij} = {}^2\Delta^{ab}_{ij}. \tag{3.32} $$

The ${}^1\Delta$ and ${}^2\Delta$ terms are

$$ {}^2\Delta^{ij}_{kl} = \sum_{a<b} {}^2T^{ab}_{ij} {}^2T^{ab}_{kl} \tag{3.33} $$

$$ {}^2\Delta^{ia}_{jb} = -\sum_{kc} {}^2T^{ac}_{jk} {}^2T^{bc}_{ik} \tag{3.34} $$

$$ {}^2\Delta^{ia}_{jk} = \sum_{b} {}^2T^{ab}_{jk} {}^1T^{b}_{i} \tag{3.35} $$

$$ {}^2\Delta^{ia}_{bc} = \sum_{j} {}^2T^{bc}_{ij} {}^1T^{a}_{j} \tag{3.36} $$

$$ {}^2\Delta^{ab}_{cd} = \sum_{i<j} {}^2T^{ab}_{ij} {}^2T^{cd}_{ij}. \tag{3.37} $$

$$ {}^1\Delta^{i}_{j} = -\sum_{a<b} \sum_{k} {}^2T^{ab}_{ik} {}^2T^{ab}_{jk} - \sum_{a} {}^1T^{a}_{i} {}^1T^{a}_{j} \tag{3.38} $$

$$ {}^1\Delta^{a}_{b} = \sum_{i<j} \sum_{c} {}^2T^{ac}_{ij} {}^2T^{bc}_{ij} - \sum_{i} {}^1T^{a}_{i} {}^1T^{b}_{i} \tag{3.39} $$

and now there are two terms that contain the reference coefficient T_0 and require topological factors to restore size-extensivity.

$$ \begin{aligned} {}^2\Delta^{ab}_{ij} &= {}^2T^{ab}_{ij} T_0 \\ &= {}^2T^{ab}_{ij} \sqrt{1 - \sum_{\substack{k<l \\ c<d}} f^{abcd}_{ijkl} ({}^2T^{cd}_{kl})^2 - \sum_{kc} f^{abc}_{ijk} ({}^1T^{c}_{k})^2} \end{aligned} \tag{3.40} $$

$$ \begin{aligned} {}^1\Delta^{a}_{i} &= {}^1T^{a}_{i} T_0 + \sum_{jb} {}^2T^{ab}_{ij} {}^1T^{b}_{j} \\ &= {}^1T^{a}_{i} \sqrt{1 - \sum_{\substack{k<l \\ c<d}} f^{cda}_{kli} ({}^2T^{cd}_{kl})^2 - \sum_{jb} f^{ab}_{ij} ({}^1T^{b}_{j})^2} \\ &+ \sum_{jb} {}^2T^{ab}_{ij} {}^1T^{b}_{j}. \end{aligned} \tag{3.41} $$

In the M parameterization [12], f_{ijkl}^{abcd} is the same as before, equal to 1 if (i, j, a, b) and (k, l, c, d) share at least two indices and zero otherwise. In a similar fashion, f_{ijk}^{abc} is set to 1 if (k, c) shares at least one index with (i, j, a, b), and f_{ij}^{ab} is set to 1 if $i = j$ or $a = b$; both factors are zero otherwise.

3.5 Concluding Remarks

The parametric 2-RDM method [12, 14, 15] is a single reference method that, like all such methods, relies upon the quality of the reference in order to provide accurate energetic predictions. It has a computational scaling that is comparable to that of coupled cluster with single and double excitations (CCSD) [19]. When the reference wavefunction is reasonably accurate and the K parameterization is used, it yields energies that are comparable to those of CCSD [14, 20–22]. By incorporating single excitations and by using the more flexible and accurate M parameterization, energies from p2-RDM typically fall [12, 23, 24] between those predicted by CCSD and the more accurate CCSD(T) [25]. However, the true strength of the method lies in the flexibility contained with the parameterization. When the reference wavefunction is of very poor quality, p2-RDM frequently outperforms [26, 27] the much more expensive CCSD(T); unlike coupled cluster methods, p2-RDM is remarkably adept at correcting the underlying reference in order to detect substantial multireference character. In the coming chapters, this ability to give accurate energies for both strongly and weakly correlated systems will be demonstrated, and extensions will be proposed to the method in order to make it more efficient and robust.

3.6 References

[1] A. J. Coleman, Rev. Mod. Phys. **35**, 668 (1963).

[2] A. J. Coleman and V. I. Yukalov, *Reduced Density Matrices: Coulson's Challenge* (Springer-Verlag, New York, 2000).

[3] R. H. Tredgold, Phys. Rev. **105**, 1421 (1957).

[4] R. Erdahl, Rep. Math. Phys. **15**, 147 (1979).

[5] R. Erdahl and B. Jin, *On Calculating Approximate and Exact Density Matrices* (Springer US, Boston, MA, 2000), pp. 57–84.

[6] D. A. Mazziotti and R. M. Erdahl, Phys. Rev. A **63**, 042113 (2001).

[7] D. A. Mazziotti, Phys. Rev. Lett. **93**, 213001 (2004).

[8] M. Nakata, H. Nakatsuji, M. Ehara, M. Fukuda, K. Nakata, and K. Fujisawa, J. Chem. Phys. **114**, 8282 (2001).

[9] G. Gidofalvi and D. A. Mazziotti, J. Chem. Phys. **126**, 024105 (2007).

[10] I. Shavitt, *The Method of Configuration Interaction* (Springer US, Boston, MA, 1977), pp. 189–275.

[11] C. D. Sherrill and H. F. Schaefer III (Academic Press, 1999), vol. 34 of *Advances in Quantum Chemistry*, pp. 143 – 269.

[12] D. A. Mazziotti, Phys. Rev. A. **81**, 062515 (2010).

[13] A. Szabo and N. S. Ostlund, *Modern Quantum Chemistry: Introduction to Advanced Electronic Structure Theory* (Dover, New York, 1996).

[14] C. Kollmar, J. Chem. Phys. **125**, 084108 (2006).

[15] D. A. Mazziotti, Phys. Rev. Lett. **101**, 253002 (2008).

[16] F. Wennmohs and F. Neese, Chem. Phys. **343**, 217 (2008).

[17] R. Ahlrichs, Comput. Phys. Commun. **17**, 31 (1979).

[18] W. Meyer, J. Chem. Phys. **58**, 1017 (1973).

[19] I. Shavitt and R. J. Bartlett, *Many-body methods in chemistry and physics: MBPT and coupled-cluster theory* (Cambridge university press, 2009).

[20] A. E. DePrince III and D. A. Mazziotti, Phys. Rev. A **76**, 042501 (2007).

[21] A. E. DePrince III, E. Kamarchik, and D. A. Mazziotti, J. Chem. Phys. **128**, 234103 (2008).

[22] A. E. DePrince III and D. A. Mazziotti, J. Chem. Phys. **130**, 164109 (2009).

[23] C. A. Schwerdtfeger, A. E. DePrince III, and D. A. Mazziotti, J. Chem. Phys. **134**, 174102 (2011).

[24] E. P. Hoy, C. A. Schwerdtfeger, and D. A. Mazziotti, Mol. Phys. **110**, 765 (2012).

[25] J. Rezac and P. Hobza, J. Chem. Theory Comput. **9**, 2151 (2013).

[26] A. M. Sand, C. A. Schwerdtfeger, and D. A. Mazziotti, J. Chem. Phys. **136**, 034112 (2012).

[27] A. J. S. Valentine and D. A. Mazziotti, J. Phys. Chem. A **117**, 9746 (2013).

CHAPTER 4

THEORETICAL PREDICTION OF THE STRUCTURES AND ENERGIES OF OLYMPICENE AND ITS ISOMERS

This chapter contains parts of an article that was originally published in the Journal of Physical Chemistry A. Reproduced with permission from [A. J. S. Valentine and D. A. Mazziotti,*J. Phys. Chem. A*, **117**, 9746 (2013)].

4.1 Introduction

The olympicene molecule, a five-ringed polyaromatic hydrocarbon (PAH), was recently synthesized [1]. PAHs have long been studied in astrophysics [2], and they are now used as molecular semiconductors [3]. Olympicene, or 6H-benzo[cd]pyrene, is related to a class of PAHs known as acenes and two-dimensional acene sheets, which represent finite approximations to graphene [4]. Of these, the linear pentacene molecule, which commonly serves as a semiconductor in field-effect transistors [5, 6], is the least compact five-ringed structure, while olympicene represents the most compact five-ringed structure (Fig. 4.1). As with all acenes, olympicene has delocalized orbitals extending over the entire π-bond network. However, unlike other acenes, olympicene is neither fully aromatic nor fully planar due to the central -CH_2- group. The two hydrogen atoms extend above and below the carbon

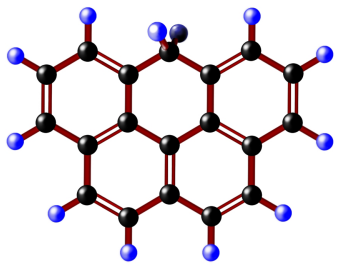

Figure 4.1: 6H-benzo[cd]pyrene, also known as olympicene.

plane, and the central carbon's sp^3-hybridization precludes its participation in the π-bond network. Acenes have previously been studied in linear [7, 8] and two-dimensional configurations. Hachmann *et al.* showed that polyradical character increases as a function of system size in linear acenes [9], and Pelzer *et al.* demonstrated a similar trend in two-dimensional acene sheets [10], while also discovering greater electron correlation in linear geometries than in nonlinear geometries.

A similar four-ringed structure, benzo[c]phenanthrene, has been known for many years [11]. Lacking the central -CH_2- group, the carbon structure of benzo[c]phenanthrene is non-planar due to steric repulsion between hydrogen atoms. In contrast, olympicene's carbon network is indeed planar. One of the out-of-plane -H functional groups in olympicene may migrate about the molecule via π-bond rearrangement, moving from the central carbon to a site located two carbons away. Instead of passing through a single transition state during this migration, the hydrogen moves along the C-C bonds, passing through two transition states and a diradical intermediate state centered above the intermediate carbon. This diradical intermediate is weakly bound, non-aromatic, and strongly correlated.

Two-electron reduced density matrix (2-RDM) methods have proven to be computationally efficient in treating strongly correlated systems [12–16]. While the active-space variational 2-RDM method was previously used to study nonlinear acene sheets [10], in this paper we use the parametric 2-RDM method [17] due to its success in treating multireference scenarios such as bond-breaking and transition-state geometries [18–20]. Olympicene was only recently synthesized, and these calculations provide predictions of its energy and properties, along with those of its isomers. We demonstrate that there exists a stable structure of olympicene, and we examine olympicene, its isomers, and the transition states connecting them. In addition, we provide information about the spin and band gaps in olympicene and compare them to those of pentacene.

4.2 Theory

4.2.1 Parametric 2-RDM method

In variational 2-RDM methods the ground-state energy is expressed as

$$E = \mathrm{Tr}({}^2K\,{}^2D), \tag{4.1}$$

where ${}^2K$ is the two-electron reduced Hamiltonian matrix which is the reduced Hamiltonian operator in a finite orbital basis set [21]. In the parametric formulation [17–20, 22–31] the second- and higher-order parts of the 2-RDM with respect to a mean-field reference are parameterized in terms of the first-order part of 2-RDM ${}^2T$. It is convenient to express the 2-RDM in terms of its cumulant expansion [32–35]

$${}^2D = 2\,{}^1D \wedge {}^1D + {}^2\Delta \tag{4.2}$$

where ${}^2\Delta$, ${}^1D$, and $\wedge$ denote the cumulant (or connected) 2-RDM, the 1-RDM, and the Grassmann wedge product [21, 36]. The second- and higher-order parts of the cumulant 2-RDM and the 1-RDM can be expressed as functionals of the 2-RDM's first-order part [22]

$${}^2\Delta \approx {}^2T + {}^2\Delta^{(2)}[{}^2T] \tag{4.3}$$

$${}^1D \approx {}^1D^{(0)} + {}^1D^{(2)}[{}^2T]. \tag{4.4}$$

With a Hartree-Fock reference wavefunction the only nonzero piece of the first-order 2-RDM is ${}^2T_{ij}^{ab}$, which is equivalent to the two-electron excitation matrix, where i and j denote occupied spin orbitals and a and b denote unoccupied (virtual) spin orbitals.

Contraction relations from the cumulant expansions of the 3- and 4-RDMs [35] yield the second-order cumulant 2-RDM and the second-order 1-RDM as functionals of the 2-RDM's

first-order part ${}^2T$ [22]:

$$
\begin{aligned}
{}^2\Delta^{ij}_{kl} &= +\sum_{a<b} {}^2T^{ab}_{ij}\,{}^2T^{ab}_{kl} && (4.5)\\
{}^2\Delta^{cd}_{ab} &= +\sum_{i<j} {}^2T^{ab}_{ij}\,{}^2T^{cd}_{ij} && (4.6)\\
{}^2\Delta^{ia}_{jb} &= -\sum_{c,k} {}^2T^{ac}_{jk}\,{}^2T^{bc}_{ik} && (4.7)
\end{aligned}
$$

and

$$
\begin{aligned}
({}^1D^{(2)})^i_j &= -\sum_{\substack{a<b\\k}} {}^2T^{ab}_{jk}\,{}^2T^{ab}_{ik} && (4.8)\\
({}^1D^{(2)})^a_b &= +\sum_{\substack{i<j\\c}} {}^2T^{ac}_{ij}\,{}^2T^{bc}_{ij}. && (4.9)
\end{aligned}
$$

Single excitations can also be explicitly included in the functionals [17, 18, 22].

While this parameterization of the 2-RDM is not N-representable, a subset of N-representability conditions, known as two-positivity conditions [37–43], can be employed to restore approximate N-representability [17, 22, 31]. The class of cumulant elements ${}^2\Delta^{ab}_{ij}$ is redefined from ${}^2T^{ab}_{ij}$ to

$$
{}^2\Delta^{ab}_{ij} = {}^2T^{ab}_{ij}\sqrt{1-\sum_{\substack{k<l\\c<d}} f^{abcd}_{ijkl}({}^2T^{cd}_{kl})^2} \qquad (4.10)
$$

where the values of f^{abcd}_{ijkl} are chosen with Cauchy-Schwarz relations from two-positivity conditions [17, 22, 31]. Further details are available in previous work [17, 22].

4.3 Applications

The parametric 2-RDM method with the M parameterization is used to investigate the olympicene molecule, its isomers, and its spin and band gaps. Similar calculations of the pentacene molecule are performed as a comparison. The results from the parametric 2-RDM

method are compared with those of conventional wavefunction methods.

4.3.1 Methodology

All calculations were performed in the Dunning-Hay (DH) double-zeta basis set. Geometries of all structures were found using 2nd-order Moeller-Plesset perturbation theory (MP2) in the GAMESS electronic structure package [44]. Transition states between nearest isomers were found via saddlepoint search and reaction pathways were confirmed by intrinsic reaction coordinate (IRC) calculations with MP2. Once structures were determined, their total energies were calculated using Hartree-Fock (HF), coupled cluster with single and double excitations (CCSD) [45], and completely renormalized coupled cluster (CR-CC(2,3)) [45, 46] in GAMESS, and the M parameterized 2-RDM (2-RDM) method [20]. All isomers and transition states of olympicene were calculated as spin-singlets. The energy of the C-H bond dissociation asymptote, benzo[*cd*]pyrene radical $C_{19}H_{11}$ and a hydrogen atom, was found by calculating the energy of the benzo[*cd*]pyrene radical in all four methods and adding the energy of a single hydrogen at infinite separation. Occupation numbers of all structures were obtained from 2-RDM and CCSD calculations. Spin and band gaps in olympicene and pentacene were obtained by calculating the total energies of their triplet, cation, and anion states at the same geometries as their respective ground states; that is, all transitions were taken to be vertical.

4.3.2 Results

The geometry of the most stable form of olympicene was successfully optimized. With the 2-RDM method, this structure is lower in energy than the C-H bond dissociation asymptote by 67.4 kilocalories per mole (kcal/mol). Of all isomers that were examined, this C_{2v}-symmetric structure is the lowest in energy by 5.7 kcal/mol. (Geometry optimization of this isomer was performed with and without C_{2v} symmetry.) It is also the most stable structure with respect to isomerization, as it is lower in energy than its transition state by 73.8 kcal/mol,

while the next most stable structure is lower in energy than its lowest transition state by 67.7 kcal/mol. Olympicene is a strongly correlated molecule with a 0.84 difference in the HONO and LUNO occupation numbers, although it is less strongly correlated than pentacene, which has a 0.70 difference in the HONO and LUNO occupation numbers.

Eleven symmetry-unique isomers were studied (Fig. 4.2), along with twelve transition states linking nearest isomers together via hydrogen migration. Of these, the six odd-numbered isomers are fully aromatic, while the five even-numbered isomers are diradicals. Ground-state energies of all 23 structures and the dissociated state, relative to the ground state of olympicene, are provided in Table 4.1 from HF, CCSD, CR-CC(2,3), and 2-RDM. Across all isomers and transition states, the 2-RDM method predicts the lowest relative energies of all methods, followed by CR-CC(2,3), CCSD, and finally HF. The relative energies of the aromatic isomers are largely consistent across all methods, as the four methods differ by approximately 3-17 kcal/mol. Results are less consistent for the transition states, where they differ by approximately 18-25 kcal/mol. Lastly, the most variable predictions are those for the highly correlated diradical isomers, where the results differ by approximately 37-44 kcal/mol. In general, the difference between the predictions of 2-RDM and CR-CC(2,3) is on the order of that between CCSD and CR-CC(2,3). This difference is most pronounced in the diradical states, where the 2-RDM method predicts relative energies that are approximately 8-11 kcal/mol lower than those of CR-CC(2,3), which are themselves lower than those of CCSD by approximately 8-11 kcal/mol. The stabilization of the diradical isomers from the 2-RDM method is qualitatively significant because it causes them to be lower in energy by 2-20 kcal/mol than hydrogen dissociation from olympicene. Unlike the diradical-isomer energies, the dissociation energies of olympicene are consistent across all methods, differing only by 1-2 kcal/mol.

The relative energies obtained from the 2-RDM method are represented in Fig. 4.3. Here we see that the aromatic isomers form deep minima on the potential energy surface, while the diradical isomers are unsurprisingly much higher in energy. The diradicals could be

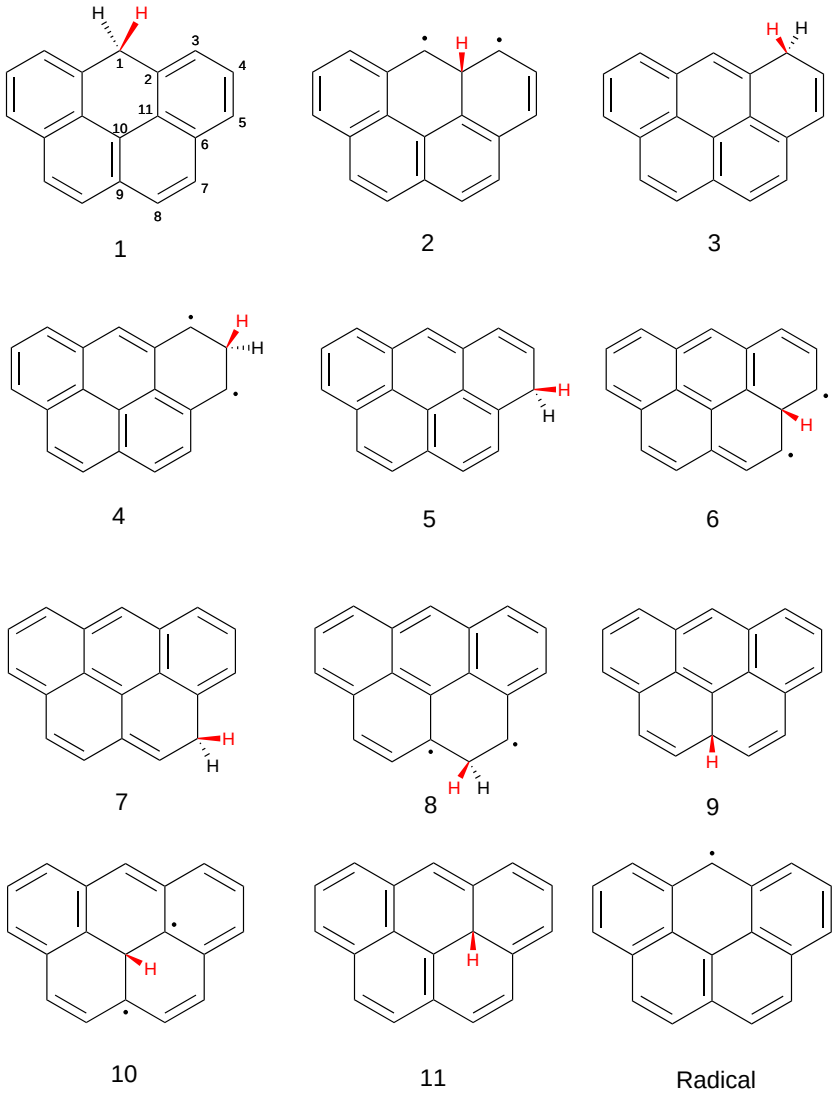

Figure 4.2: Olympicene, its isomers, and the benzo[*cd*]pyrene radical.

Table 4.1: Ground-state energies [kilocalories per mole (kcal/mol)], relative to the ground state of olympicene, of all isomers, transition states, and the benzo[*cd*]pyrene radical plus hydrogen (Rad+H) dissociation asymptote are presented from HF, CCSD, CR-CC(2,3), and parametric 2-RDM methods in the Dunning-Hay basis. The notation $x \rightarrow y$ represents the transition state between structures x and y.

	Isomer energies relative to the ground state (kcal/mol)			
Structure	HF	CCSD	CR-CC(2,3)	2-RDM
1	0.000	0.000	0.000	0.000
1→2	98.964	82.410	76.698	73.758
2	105.621	81.048	71.384	62.185
2→3	102.640	86.838	81.589	78.869
3	10.017	7.828	7.445	6.796
3→4	93.727	79.927	75.114	73.249
4	89.820	70.799	61.394	50.390
4→5	94.865	80.699	75.771	73.318
5	8.450	6.482	6.229	5.660
5→6	101.505	86.462	81.197	78.572
6	102.858	82.824	73.969	65.241
6→7	109.321	94.241	88.594	86.414
7	24.607	20.316	20.013	17.680
7→8	98.280	85.544	80.519	78.000
8	85.470	68.670	57.620	47.297
8→9	100.752	86.629	82.077	80.225
9	37.943	27.442	26.950	24.521
9→10	105.256	91.487	87.069	85.642
10	101.773	81.820	72.870	64.415
10→11	107.350	94.126	89.963	89.130
11	47.949	35.053	34.674	30.554
2→11	109.184	95.819	91.558	90.504
6→11	106.764	94.191	90.060	89.285
Rad+H	68.154	69.432	68.019	67.399

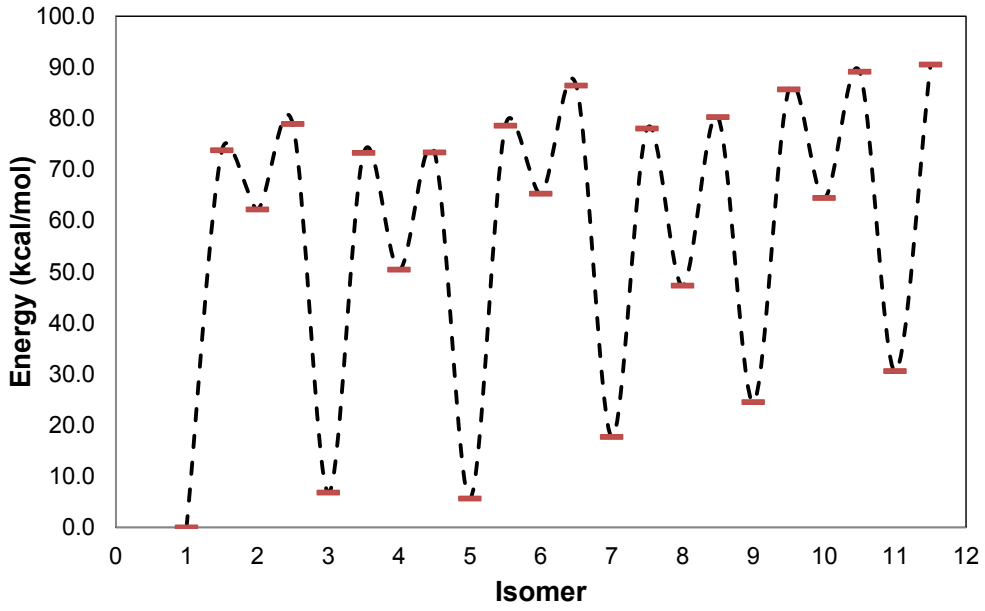

Figure 4.3: Isomer and transition-state energies relative to the ground state, calculated from the parametric 2-RDM method in the Dunning-Hay basis. The isomer labels are defined in Fig. 4.2.

thought of as shallow intermediates on the reaction pathway, existing briefly as a π-bond breaks during the migration of a hydrogen from one aromatic isomer to another. We also see a general trend of increasing energy and decreasing stability among aromatic isomers as the hydrogen migrates around and then into the molecule. This trend may be explained by Clar's sextet rule, which states that ringed aromatic structures with more disjoint π-sextets are more stable and lower in energy than those with fewer sextets. The isomers in Fig. 4.2 are shown in their Clar form, where isomers 1, 3, and 5 can form two π-sextets, while isomers 7, 9, and 11 may only form one. In general, the aromaticity becomes increasingly restricted as the hydrogen moves around the molecule, changing from four aromatic rings in an arch-shape in structure 1 to only two aromatic rings in structure 11, with energy increasing as the aromaticity is restricted further.

From the occupation numbers provided in Table 4.1, we can see that the 2-RDM method successfully predicts near-diradical character in the non-aromatic isomers, with differences in HONO and LUNO occupation numbers of approximately 0.1-0.25. In contrast, CCSD

Table 4.2: Occupation numbers of the highest-occupied (HONO) and lowest-unoccupied (LUNO) natural orbitals of all isomers and transition states are presented from CCSD and the parametric 2-RDM methods in the Dunning-Hay basis.

	Natural-orbital occupation numbers			
	CCSD		2-RDM	
Structure	n_{HONO}	n_{LUNO}	n_{HONO}	n_{LUNO}
1	0.9451	0.0503	0.9196	0.0748
1→2	0.9178	0.0765	0.8044	0.1854
2	0.8679	0.1268	0.5919	0.3985
2→3	0.9236	0.0708	0.8216	0.1670
3	0.9391	0.0570	0.9029	0.0923
3→4	0.9269	0.0657	0.8443	0.1411
4	0.8674	0.1272	0.5518	0.4398
4→5	0.9259	0.0664	0.8314	0.1541
5	0.9401	0.0563	0.9070	0.0885
5→6	0.9273	0.0647	0.8198	0.1680
6	0.8928	0.1010	0.6181	0.3721
6→7	0.9297	0.0641	0.8342	0.1517
7	0.9328	0.0635	0.8806	0.1146
7→8	0.9294	0.0625	0.8279	0.1582
8	0.8691	0.1262	0.5584	0.4357
8→9	0.9310	0.0629	0.8522	0.1352
9	0.9370	0.0595	0.8961	0.1000
9→10	0.9372	0.0529	0.8581	0.1235
10	0.8997	0.0927	0.5955	0.3912
10→11	0.9375	0.0538	0.8799	0.1020
11	0.9337	0.0632	0.8761	0.1200
2→11	0.9367	0.0569	0.8751	0.1129
6→11	0.9374	0.0561	0.8797	0.1079

captures much less of the multi-reference character of these diradicals, with HONO-LUNO occupation-number gaps ranging from approximately 0.75 to 0.8. In general, the 2-RDM method captures more of the multireference correlation than does CCSD in all structures. In addition, the 2-RDM method predicts a general trend of decreasing HONO-LUNO gaps among aromatic isomers as the aromaticity is restricted, supporting the trend of increasing energy observed in Fig. 4.3. Conversely, CCSD predicts no substantial change in occupation numbers as aromaticity is restricted, again suggesting that the 2-RDM method is better suited to treat the multireference character of this molecule.

The energies of all isomers and transition states, relative to the C-H bond dissociation asymptote, are plotted in Fig. 4.4 from 2-RDM and CCSD. Predictions for the relative energies of aromatic isomers are largely consistent between the two methods, while 2-RDM predicts slightly lower energies for the transition states than does CCSD. The greatest difference occurs in the non-aromatic isomers, where 2-RDM predicts that all five such isomers are lower in energy than the dissociation asymptote. In contrast, only one stable non-aromatic isomer is predicted by CCSD. Incorporating the triples corrections from CR-CC(2,3) brings the energies of the diradical states closer to those from 2-RDM, although three of those isomers are still predicted to be higher in energy than the dissociation asymptote. While CR-CC(2,3) generally captures more dynamic correlation energy than does the 2-RDM method, the reduced density matrix approach captures significantly more static correlation energy. In the case of the diradical states, the increased static correlation from the 2-RDM method is sufficient to predict substantially different results for the stability of olympicene's isomers.

Barrier energies with respect to hydrogen migration are presented in Table 4.3 from CCSD, CR-CC(2,3), and 2-RDM. Among the aromatic isomers (the first half of the table), the 2-RDM method most often predicts the smallest barrier heights, and always yields lower barriers than does CCSD. In contrast, the 2-RDM method predicts higher barriers than CCSD and CR-CC(2,3) for every diradical isomer (the second half of the table). This dichotomy is a result of the multireference character captured by the 2-RDM method. As shown above, polyradical character of the molecule increases from aromatic isomers to transition states to diradical isomers, and the increased static correlation leads 2-RDM to lower the energies of more correlated states relative to less correlated states. This has the ultimate effect of lowering the barriers for the aromatic isomers and greatly stabilizing the diradical isomers. Similar results have been observed in recent parametric 2-RDM calculations on the stability of oxywater [29] and the rotational barrier separating *cis* and *trans* diazene [20].

To investigate olympicene's potential utility in technology, we computed the spin and band gaps of olympicene from all four methods shown in Table 4.4 with those of pen-

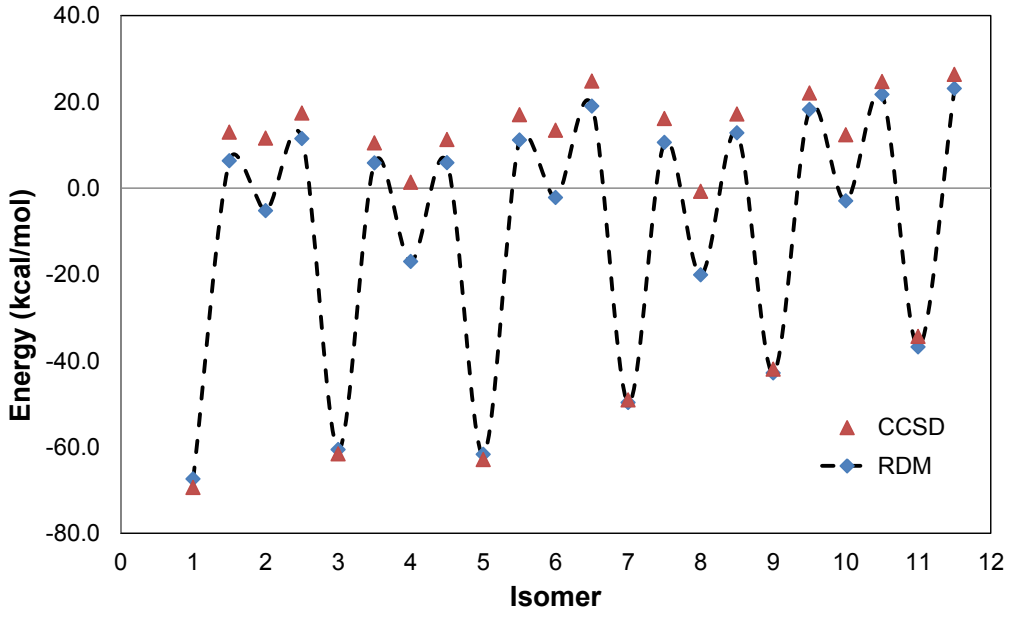

Figure 4.4: Isomer and transition state energies relative to the benzo[*cd*]pyrene radical and a hydrogen atom, obtained from CCSD and the parametric 2-RDM method in the Dunning-Hay basis set. The 2-RDM method predicts relative diradical energies that are approximately 8-11 kcal/mol lower than those of CR-CC(2,3), which are themselves lower than those of CCSD by approximately 8-11 kcal/mol. The stabilization of the diradical isomers from the 2-RDM method is qualitatively significant because it causes them to be lower in energy than the dissociation products by 2-20 kcal/mol.

Table 4.3: Barrier energies [kilocalories per mole (kcal/mol)] with respect to hydrogen migration for each isomer are presented here from CCSD, CR-CC(2,3), and the parametric 2-RDM methods in the Dunning-Hay basis set. The transition $x \rightarrow y$ signifies the height, relative to x, of the barrier separating x and y. Transitions are ordered from largest to smallest barrier height.

	Barrier energies (kcal/mol)				Barrier energies (kcal/mol)		
Transition	CCSD	CR-CC(2,3)	2-RDM	Transition	CCSD	CR-CC(2,3)	2-RDM
1→2	82.410	76.698	73.758	8→7	16.874	22.898	30.703
5→6	79.980	74.969	72.912	2→11	14.771	20.173	23.319
3→2	79.010	74.144	72.072	10→11	12.306	17.093	24.715
7→6	73.925	68.580	68.733	6→11	11.367	16.091	24.045
5→4	74.217	69.542	67.658	4→5	9.900	14.376	22.928
3→4	72.098	67.668	66.452	4→3	9.128	13.719	22.858
9→10	64.045	60.119	61.121	10→9	9.666	14.199	21.227
7→8	65.228	60.505	60.320	6→7	11.417	14.625	21.173
11→2	60.766	56.884	59.950	2→3	5.791	10.205	16.684
11→10	59.073	55.289	58.576	6→5	3.638	7.229	13.331
9→8	59.187	55.127	55.704	2→1	1.362	5.313	11.574
8→9	17.959	24.457	32.927				

tacene given as a reference. All methods predict a significantly larger singlet-triplet gap in olympicene than in pentacene. Only the 2-RDM method predicts a plausibly stable triplet state in olympicene, which is approximately 14 kcal/mol lower in energy than the dissociation asymptote. All methods likewise predict a larger ionization energy (IE) and a lower electron affinity (EA) in olympicene than in pentacene, yielding a much greater fundamental gap (IE-EA) for olympicene. This implies that olympicene is potentially a less suitable conductor than pentacene.

4.4 Discussion and Conclusion

The olympicene molecule, a modification of pentacene, was recently synthesized [1]. Similar to pentacene, olympicene is a five-ringed polyaromatic hydrocarbon. While pentacene is the least compact five-ringed structure possible, olympicene is the most compact possible structure. Unlike pentacene, olympicene has two hydrogen atoms extending above and below the plane, and thus numerous isomers of olympicene are possible. We find that several stable

Table 4.4: Spin and band gaps (kcal/mol) in olympicene and pentacene, as well as the C-H bond dissociation energy of olympicene, are presented here from Hartree-Fock (HF), CCSD, CR-CC(2,3), and the parametric 2-RDM methods in the Dunning-Hay basis. The singlet-triplet gap is the difference in energies between the triplet and singlet states of each molecule. The fundamental band gap IE-EA is the difference between the ionization energy IE=E_{cation}-E_0 and the electron affinity EA=E_0-E_{anion}, where E_0 is the energy of the ground state.

	Energy gaps (kcal/mol)				
Molecule	Energy Gap	HF	CCSD	CR-CC(2,3)	2-RDM
Olympicene	Singlet-Triplet	77.747	70.920	68.013	53.234
	IE	155.154	163.336	161.247	162.057
	EA	-26.984	-19.223	-17.462	-18.837
	IE-EA	182.138	182.560	178.709	180.894
	Dissociation	68.154	69.432	68.019	67.399
Pentacene	Singlet-Triplet	22.175	28.417	28.498	25.215
	IE	128.932	142.232	141.279	145.450
	EA	7.630	9.777	10.329	5.756
	IE-EA	121.302	132.455	130.951	139.695

isomers of olympicene exist, and that its most stable isomer is the C_{2v}-symmetric structure. Pentacene's success as a organic semiconductor suggests that olympicene might likewise possess useful electronic properties. Calculations reveal that olympicene has less strong correlation than pentacene, which is consistent with previous results showing linear acenes to be more strongly correlated than nonlinear acenes [10].

We find that the isomers of olympicene may be divided into two categories: aromatic and diradical. Olympicene may isomerize between these different structures as one of the out-of-plane hydrogen atoms migrates around the molecule. A π-bond breaks during this isomerization, giving diradical isomers that are intermediates along the reaction pathway. We find that these diradicals are unsurprisingly much higher in energy than the aromatic isomers, and the parametric 2-RDM method is able to capture most of their diradical character, as confirmed by natural occupation numbers. In addition, aromaticity becomes increasingly restricted during the hydrogen migration, with a corresponding increase in energy and in polyradical character. Despite the higher energies of the diradical isomers, however, the parametric 2-RDM method indicates that they are 2-20 kcal/mol more stable than C-H

bond dissociation asymptote, which raises the possibility of their synthesis.

Several important chemical properties, such as polyradical character and energy gaps, can only be fully captured with accurate treatments of strong correlation. The analysis of olympicene's many isomers, with their varying degrees of radical character, therefore requires electronic structure methods with a robust ability to treat medium and strong electron correlation, both static and dynamic. Unlike the traditional single-reference wavefunction methods we employed, the parametric 2-RDM method [17] was able to capture a substantial portion of the polyradical character of olympicene and its isomers, despite being constructed from a single slater determinant. Likewise, 2-RDM was able to observe diradical character in the non-aromatic isomers of olympicene, while coupled-cluster methods predicted almost no such behavior. Finally, only the 2-RDM method predicts stable forms of all five non-aromatic (diradical) isomers studied, all at a lower computational cost than CCSD or CR-CC(2,3). The calculations with olympicene demonstrate the applicability of the parametric 2-RDM method to a broad range of electron correlation problems in chemistry and physics.

4.5 References

[1] A. Mistry, B. Moreton, B. Schuler, F. Mohn, G. Meyer, L. Gross, A. Williams, P. Scott, G. Costantini, and D. J. Fox, Chem. Eur. J. **21**, 2011 (2015).

[2] A. G. G. M. Tielens, Annu. Rev. Astron. Astophys. **46**, 289 (2008).

[3] Y. Geerts, G. Klärner, and K. Müllen, *Electronic Materials: The Oligomer Approach* (Wiley-VCH, Weinheim, Germany, 1998).

[4] A. Geim and K. Novoselov, S. Nat. Mater. **6**, 183 (2007).

[5] N. Koch, ChemPhysChem **8**, 1438 (2007).

[6] T. Hasegawa and J. Takeya, Sci. Technol. Adv. Mater. **10**, 024314 (2009).

[7] G. Gidofalvi and D. A. Mazziotti, J. Chem. Phys. **129**, 134108 (2008).

[8] M. Bendikov, H. M. Duong, K. Starkey, K. N. Houk, E. A. Carter, and F. Wudl, J. Am. Chem. Soc. **126**, 7416 (2004).

[9] J. Hachmann, J. Dorando, M. Aviles, and G. K.-L. Chan, J. Chem. Phys. **127**, 134309 (2007).

[10] K. Pelzer, L. Greenman, G. Gidofalvi, and D. A. Mazziotti, J. Phys. Chem. A **115**, 56325640 (2011).

[11] J. Cook, J. Chem. Soc. pp. 2524–2528 (1931).

[12] D. A. Mazziotti, Chem. Rev. **112**, 224 (2012).

[13] J. R. Hammond and D. A. Mazziotti, Phys. Rev. A **73**, 062505 (2006).

[14] C. A. Schwerdtfeger and D. A. Mazziotti, J. Chem. Phys. **130**, 224102 (2009).

[15] A. Sinitskiy, L. Greenman, and D. A. Mazziotti, J. Chem. Phys. **133**, 014104 (2010).

[16] L. Greenman and D. A. Mazziotti, J. Chem. Phys. **133**, 164110 (2010).

[17] D. A. Mazziotti, Phys. Rev. Lett. **101**, 253002 (2008).

[18] A. E. DePrince III and D. A. Mazziotti, Phys. Rev. A **76**, 042501 (2007).

[19] A. E. DePrince III, E. Kamarchik, and D. A. Mazziotti, J. Chem. Phys. **128**, 234103 (2008).

[20] C. A. Schwerdtfeger, A. E. DePrince III, and D. A. Mazziotti, J. Chem. Phys. **134**, 174102 (2011).

[21] D. A. Mazziotti, Phys. Rev. A **57**, 4219 (1998).

[22] D. A. Mazziotti, Phys. Rev. A. **81**, 062515 (2010).

[23] A. E. DePrince III and D. A. Mazziotti, J. Phys. Chem. B **112**, 16158 (2008).

[24] A. E. DePrince III and D. A. Mazziotti, J. Chem. Phys. **130**, 164109 (2009).

[25] A. E. DePrince III and D. A. Mazziotti, J. Chem. Phys. **132**, 034110 (2010).

[26] A. E. DePrince III and D. A. Mazziotti, J. Chem. Phys. **133**, 034112 (2010).

[27] C. A. Schwerdtfeger and D. A. Mazziotti, J. Phys. Chem. A **115**, 12011 (2011).

[28] A. Sand, C. A. Schwerdtfeger, and D. A. Mazziotti, J. Chem. Phys. **136**, 034112 (2012).

[29] E. Hoy, C. A. Schwerdtfeger, and D. A. Mazziotti, Mol. Phys. **110**, 765 (2012).

[30] A. E. DePrince III and D. A. Mazziotti, Mol. Phys. **110**, 1917 (2012).

[31] C. Kollmar, J. Chem. Phys. **125**, 084108 (2006).

[32] D. A. Mazziotti, Chem. Phys. Lett. **289**, 419 (1998).

[33] D. A. Mazziotti, Int. J. Quantum Chem. **70**, 557 (1998).

[34] D. A. Mazziotti, Phys. Rev. A **60**, 3618 (1999).

[35] D. A. Mazziotti, Chem. Phys. Lett. **326**, 212 (2000).

[36] W. Slebodzinski, *Exterior Forms and their Applications* (Polish Scientific Publishers, Warsaw, 1970).

[37] D. A. Mazziotti, ed., *Reduced-Density-Matrix Mechanics: With Application to Many-electron Atoms and Molecules*, vol. 134 of *Advances in Chemical Physics* (Wiley, New York, 2007).

[38] C. Garrod and J. Percus, J. Math. Phys. **5**, 1756 (1964).

[39] D. A. Mazziotti and R. M. Erdahl, Phys. Rev. A **63**, 042113 (2001).

[40] M. Nakata, H. Nakatsuji, M. Ehara, M. Fukuda, K. Nakata, and K. Fujisawa, J. Chem. Phys. **114**, 8282 (2001).

[41] Z. Zhao, B. J. Braams, H. Fukuda, M. L. Overton, and J. K. Percus, J. Chem. Phys. **120**, 2095 (2004).

[42] D. A. Mazziotti, Phys. Rev. A **65**, 062511 (2002).

[43] D. A. Mazziotti, Phys. Rev. A **74**, 032501 (2006).

[44] M. W. Schmidt, K. K. Baldridge, J. A. Boatz, S. T. Elbert, M. S. Gordon, J. H. Jensen, S. Koseki, N. Matsunaga, K. A. Nguyen, S. Su, T. L. Windus, M. Dupuis, and J. A. Montgomery, J. Comput. Chem. **14**, 1347 (1993).

[45] P. Piecuch, S. A. Kucharski, K. Kowalski, and M. Musial, Comput. Phys. Commun. **149**, 71 (2002).

[46] P. Piecuch and M. Wloch, J. Chem. Phys. **123**, 224105 (2005).

CHAPTER 5
ANALYTICAL NUCLEAR DERIVATIVES FOR THE PARAMETRIC TWO-ELECTRON REDUCED-DENSITY-MATRIX METHOD

5.1 Introduction

In quantum chemistry, the electronic Schrödinger equation is solved in order to find the electronic energy, typically using the many-electron wavefunction as the primary variable. However, because the Hamiltonian contains only pairwise interactions between particles, it was observed by Coleman in 1951 that the energy may equally be expressed using the two-electron reduced density matrix (2-RDM) [1]. The set of all possible 2-RDMs is much larger than the set of all N-electron wavefunctions, and thus direct minimization of the energy with respect to the 2-RDM yields energies that are much too low. Constraints or *N-representability* conditions are required for the 2-RDM to represent a physically realistic N-electron density matrix [2]. There are currently several categories of 2-RDM methods, with differing mechanisms for enforcing approximate *N-representability*. The contracted Schrödinger equation [3–5] or its anti-Hermitian part [6] are root-finding algorithms that begin with an initial wavefunction guess. The variational 2-RDM method [7–9] directly minimizes the energy with respect to the 2-RDM while enforcing necessary N-representability conditions. Lastly, the parametric 2-RDM (p2-RDM) method [10, 11] features a parameterization, derived from configuration interaction (CI) methods [12], that preserves approximate N-representability. Parametric 2-RDM has proven particularly adept at treating strongly correlated systems where multireference correlation plays an important role, such as transition states [13, 14] or bond-dissociation pathways [15, 16].

Geometry optimization is the process of finding the minimum-energy structure of a molecule. This minimization can be performed efficiently using quasi-Newton methods,

provided that the exact nuclear gradient is known at each geometry step. The gradient may be found numerically, but this requires at least two complete electronic structure calculations for each of the $3N$-6 nuclear degrees of freedom, making the evaluation very costly. If the gradient can be found analytically, only one electronic structure calculation is required per geometry step, greatly accelerating the optimization [17]. For this reason, analytical gradients have been implemented for many quantum chemical methods, including coupled cluster [18], configuration interaction [19], density functional theory [20], and density-matrix renormalization group [21] methods. It was observed [22] early on that analytical gradients are also possible for the parametric 2-RDM method. Initial attempts to implement such gradients for p2-RDM used numerical gradients of electron integrals in the molecular orbital (MO) basis [22, 23]. However, MOs can easily change in either phase or energetic ordering, even for very slight nuclear perturbations, and therefore these gradients proved insufficiently stable to be of general practical use. Geometry optimizations for p2-RDM have since featured numerical nuclear gradients [13, 16, 24], limiting the size of systems that could be treated. In this work, we will for the first time present full analytical nuclear gradients for p2-RDM, and will discuss both their efficacy and implementation.

5.2 Theory

5.2.1 Parametric 2-RDM method

The wavefunction ansatz for configuration interaction with double excitations (CID) is given by

$$|\Psi\rangle = T_0|\Phi_0\rangle + \sum_{\substack{i<j \\ a<b}} {}^2T_{ij}^{ab}|\Phi_{ij}^{ab}\rangle \tag{5.1}$$

where $|\Phi_0\rangle$ is the reference wavefunction (typically obtained from Hartree-Fock) and $|\Phi_{ij}^{ab}\rangle$ is the Slater determinant where two electrons have been excited from the occupied orbitals i and j into the virtual orbitals a and b. The Latin letters $\{i, j, k, l\}$ in this work will refer to

orbitals that are occupied in the reference, the letters $\{a, b, c, d\}$ will refer to virtual orbitals, and the letters $\{p, q, r, s\}$ will refer to any generic orbitals. Direct minimization of the energy

$$E = \langle \Psi | H | \Psi \rangle \tag{5.2}$$

with respect to the coefficients T_0 and $\{{}^2T_{ij}^{ab}\}$ will yield the CID wavefunction, provided that the wavefunction is normalized, or

$$T_0 = \sqrt{1 - \sum_{\substack{i<j \\ a<b}} ({}^2T_{ij}^{ab})^2}. \tag{5.3}$$

This method may equivalently be represented using two-electron reduced density matrices (2-RDM) by directly contracting the wavefunction ansatz in Eq. 5.1 onto a 2-RDM using Wick's Theorem [10–12]. The exact expression for ${}^2D_{rs}^{pq}$ depends on the number of orbitals in $\{p, q, r, s\}$ that are occupied and virtual, respectively. The fully unoccupied portion of the 2-RDM, for example, may be expressed in terms of $\{{}^2T_{ij}^{ab}\}$ as

$${}^2D_{ab}^{cd} = \sum_{i<j} {}^2T_{ij}^{ab} {}^2T_{ij}^{cd}. \tag{5.4}$$

Expressions for other portions of the 2-RDM may be found in previous work [25]. When the energy of the CID 2-RDM

$$E = \mathrm{Tr}({}^2K\,{}^2D) \tag{5.5}$$

is minimized with respect to the same variables, an identical energy to CID is obtained, where ${}^2K$ is the two-electron reduced Hamiltonian matrix. The variational condition satisfied by this minimization is given by

$$\frac{\partial E}{\partial {}^2T_{ij}^{ab}} = 0 \forall_{i,j,a,b}. \tag{5.6}$$

It is well known that truncated CI methods such as CID are not size-extensive. A

correlated method is *size extensive* if its correlation energy increases linearly with the size of a molecule. This lack of size extensivity arises from a single class of 2-RDM elements

$$ {}^2D_{ij}^{ab} = T_0 {}^2T_{ij}^{ab} \tag{5.7} $$

due to the normalization condition in Eq. 5.3 containing unconnected terms [10–12]. The density matrix formulation of CID may be rendered size extensive by the insertion of a topological factor f_{ijkl}^{abcd} into the normalization condition, converting the expression in Eq. 5.4 to

$$ {}^2D_{ij}^{ab} = {}^2T_{ij}^{ab} \sqrt{1 - \sum_{\substack{k<l \\ c<d}} f_{ijkl}^{abcd} ({}^2T_{kl}^{cd})^2} \tag{5.8} $$

If f is set to 1 for all values of $\{ijklabcd\}$, the CID method is recovered, whereas if it is set to zero, the method is equivalent to the coupled-electron pair approximation (CEPA) [26, 27]. Several choices of f have been proposed, both in the context of extensions to CEPA and the parametric 2-RDM method (our work). The p2-RDM family of methods is distinct from the earlier CEPA methods in that it employs a specific, more accurate class of functions, derived from N-representability conditions on the 2-RDM [10]. One of the most accurate functionals is the M parameterization, wherein f is equal to 1 if $\{klcd\}$ share at least two indices with $\{ijab\}$, and 0 otherwise [10, 25].

5.2.2 Nuclear Derivatives

Differentiating the energy in Eq. 5.5 with respect to some nuclear perturbation R yields two terms

$$ \frac{dE}{dR} = \mathrm{Tr}(\frac{d^2K}{dR} {}^2D) + \mathrm{Tr}({}^2K \frac{d^2D}{dR}) \tag{5.9} $$

which will be treated individually in the following sections.

Nuclear Derivatives of the 2-RDM

The second term in Eq. 5.9 may be expressed as

$$\mathrm{Tr}({}^2K\frac{d^2D}{dR}) = \sum_{pqrs} {}^2K^{pq}_{rs}(\frac{d^2D}{dR})^{rs}_{pq}. \tag{5.10}$$

Because the 2-RDM is a function only of $\{{}^2T^{ab}_{ij}\}$, its derivative may be expressed using the chain rule

$$\mathrm{Tr}({}^2K\frac{d^2D}{dR}) = \sum_{pqrs} {}^2K^{pq}_{rs} \sum_{\substack{i<j \\ a<b}} \frac{\partial^2 D^{pq}_{rs}}{\partial^2 T^{ab}_{ij}} \frac{d^2T^{ab}_{ij}}{dR}. \tag{5.11}$$

Rearranging the order of summation gives

$$\mathrm{Tr}({}^2K\frac{d^2D}{dR}) = \sum_{\substack{i<j \\ a<b}} \frac{d^2T^{ab}_{ij}}{dR} \sum_{pqrs} {}^2K^{pq}_{rs} \frac{\partial^2 D^{pq}_{rs}}{\partial^2 T^{ab}_{ij}}. \tag{5.12}$$

However, examining the term within the second summation, we observe that

$$\sum_{pqrs} {}^2K^{pq}_{rs} \frac{\partial^2 D^{pq}_{rs}}{\partial^2 T^{ab}_{ij}} = \frac{\partial E}{\partial^2 T^{ab}_{ij}} \tag{5.13}$$

which, as per the variational condition in Eq. 5.6, is 0 for all $\{i, j, a, b\}$. Consequently, the first derivative of the 2-RDM does not contribute to the first derivative of the energy, which is generally true for any method which employs a variational condition. The nuclear gradient therefore depends only on ${}^2D$ and the derivative of ${}^2K$.

Nuclear Derivatives of the Reduced Hamiltonian Matrix

The nuclear first derivative of the energy for the parametric 2-RDM method depends only on the derivative of the reduced Hamiltonian matrix ${}^2K$. This matrix contains the one- and two-electron integrals, which are given in the basis of molecular orbitals (MOs). MOs are

themselves linear combinations of atomic orbitals (AOs), defined as

$$|\phi_i\rangle = \sum_{i\mu} C^{\dagger}_{i\mu}|\chi_\mu\rangle \tag{5.14}$$

where C is the MO coefficient matrix and the Greek letters $\{\mu, \nu\}$ denote AOs. The reduced Hamiltonian matrix in the MO basis may be transformed from ${}^2K$ in the AO basis by

$${}^2_{MO}K^{pq}_{rs} = (C^{\dagger}_{p\alpha}C^{\dagger}_{q\beta})\,{}^2_{AO}K^{\alpha\beta}_{\gamma\delta}(C_{\gamma r}C_{\delta s}). \tag{5.15}$$

The derivative of this matrix, then, will depend on the derivatives of both the bare AO integrals and the MO expansion coefficients C. The former may be obtained directly from any software package that evaluates electron integrals, while the latter must be solved for. Expressing $\frac{dC}{dR}$ in terms of the initial expansion coefficients

$$\frac{dC_{\mu i}}{dR} = \sum_j U_{ij}C^{\dagger}_{j\mu} \tag{5.16}$$

the total derivative of ${}^2K$ can be written as

$$\frac{d^2K^{kl}_{ij}}{dR} = \sum_{\alpha\beta\gamma\delta} C^{\dagger}_{i\alpha}C^{\dagger}_{j\beta}\frac{d^2K^{\gamma\delta}_{\alpha\beta}}{dR}C_{\gamma k}C_{\delta l} + \sum_{m\alpha\beta\gamma\delta}\Big[U_{mi}C^{\dagger}_{i\alpha}C^{\dagger}_{j\beta}\,{}^2K^{\gamma\delta}_{\alpha\beta}C_{\gamma k}C_{\delta l} + 3 \text{ other terms}\Big] \tag{5.17}$$

where there are four terms in the second summation because there is a derivative for each of the four C coefficients. In general, the MO coefficients C are coupled to the other wave-function parameters, making the process of determining U non-trivial. If one uses canonical HF MOs, however, U may be found by solving the coupled-perturbed Hartree-Fock (CPHF) equations [28]. In the case of restricted Hartree-Fock (RHF) references for singlet states, U

has the following expression

$$U_{ij} = \frac{1}{\epsilon_j - \epsilon_i} \left[\sum_{k}^{virt} \sum_{l}^{d.o.} A_{ij}^{kl} U_{kl} + B_{ij} \right] \tag{5.18}$$

where

$$A_{ij}^{kl} = 4^2V_{ij}^{kl} - {}^2V_{ik}^{jl} - {}^2V_{il}^{jk} \tag{5.19}$$

$$B_{ij} = \frac{\partial F_{ij}}{\partial R} - \frac{\partial S_{ij}}{\partial R}\epsilon_j - \sum_{kl} \frac{\partial S_{kl}}{\partial R}(2^2V_{ij}^{kl} - V_{ik}^{jl}) \tag{5.20}$$

Here F is the Fock matrix, S the overlap matrix in the MO basis, $\{\epsilon_i\}$ the Hartree-Fock MO energies, and *d.o.* means a summation over doubly-occupied MOs. Equation 5.18 may be solved iteratively to find U, at a computational cost comparable to a single HF calculation. This process must be performed for each nuclear degree of freedom (DOF). As seen in Eq. 5.18, the derivative matrix ${}_{AO}^{2}K$ must be rotated into the MO basis for each DOF, which scales as r^6, where r is the number of MOs. Analytical gradients may be rendered computationally cheaper still by implementing the Z-vector method [29], an alternative way of solving the CPHF equations that instead involves rotating ${}^2D$ into the AO basis, reducing the number of orbital rotations from $3N$ to 1 for each geometry step. For a more detailed discussion of the CPHF equations and the more efficient Z-vector method of solving them, see Ref. [30].

5.3 Applications

Analytical gradients are implemented for the parametric 2-RDM method. Benchmark calculations to test their efficacy are presented. These gradients are then applied to the optimization of *trans*-polyacetylene chains.

5.3.1 Methodology

The parametric 2-RDM method was used to find the optimized geometries of a suite of molecules in a series of basis sets. Hartree-Fock and the p2-RDM method were implemented by the authors in C++. Atomic orbital integrals and their derivatives were obtained from the LIBINT package of the Valeev group [31]. Energy gradients were evaluated using the Z-vector method [29]. Energy minimization, during either single-point p2-RDM calculations or geometry optimizations, was performed using L-BFGS [32], implemented with the ALGLIB package [33]. Core orbitals (that is, all occupied MOs not in the valence shell) were frozen during all p2-RDM calculations. Geometry optimizations were carried out in Cartesian coordinates; where necessary, the relevant nuclear degrees of freedom were frozen for the atom nearest the molecular center of mass to prevent translation of the molecule.

5.3.2 Results

To highlight the benefits of using analytical rather than numerical nuclear gradients, we performed a series of geometry optimizations for a variety of small molecules and basis sets [34], presented in Table 5.1. It is readily apparent that analytical gradients substantially reduce the CPU times of geometry optimizations in nearly every instance. This increase in computational efficiency is possible because numerical gradients require two full p2-RDM single-point calculations for each nuclear degree of freedom (DOF), whereas the analytical gradients require only a single single-point calculation per geometry step. Consequently, the gap between the two methods grows as the number of nuclear DOF increases; even NH_3, which has only 5 unfrozen DOF, sees a runtime reduction of almost 7 hours in the cc-pVQZ basis. In the one instance where the numerical gradients are faster, CO in the cc-pVDZ basis, there is only a single nuclear DOF, and the electronic DOF are so few that both methods finish almost immediately. Analytical gradients will yield greater benefits for larger molecular systems, allowing the p2-RDM method to treat molecular geometries that were previously inaccessible.

Table 5.1: A comparison of CPU times for geometry optimizations using either analytical or numerical gradients from the parametric 2-RDM method. The number of unfrozen nuclear degrees of freedom (nuc. DOF) are given in parentheses for each species. Results are presented in three basis sets for each molecule, with the number of molecular orbitals (MOs) given. CO, H_2O, and CH_4 were given the point group C_{2v}, while NH_3 was examined in the C_s point group. The runtimes for geometry optimizations are greatly decreased by using analytical gradients.

Molecule (Nuc. DOF)	Basis	MOs	Time: Numerical (s)	Time: Analytical (s)
CO (1)	cc-pVDZ	28	2.5	5.2
	cc-pVTZ	60	41.5	29.4
	cc-pVQZ	110	872	668
H_2O (2)	cc-pVDZ	24	2.9	1.7
	cc-pVTZ	58	65.0	40.4
	cc-pVQZ	115	2031	1080
CH_4 (4)	cc-pVDZ	34	5.8	3.1
	cc-pVTZ	86	604	166
	cc-pVQZ	175	12467	3626
NH_3 (5)	cc-pVDZ	29	12.6	7.1
	cc-pVTZ	72	1745	329
	cc-pVQZ	145	34917	9906

As a further demonstration of the abilities of analytical gradients, the parametric 2-RDM method was used to optimize the geometries of *trans*-polyacetylene (PA), $H[C_2H_2]_NH$, for N of 2, 4, 6, and 8. The bond length alternation (BLA) of this species, defined as the difference in length between adjacent double and single bonds, is notoriously difficult for theoretical methods to predict accurately [35]. Experiment suggests that the BLA in the infinite polymer limit lies between 0.08 and 0.09 Å [36, 37], while theoretical studies have suggested values ranging from 0.05 to 0.12 Å [21, 35, 38, 39]. Even among coupled cluster methods, CCSD(T) accurately predicts a BLA around 0.085 Åin the infinite limit, while CCSD predicts a BLA that is much higher at 0.0995 Å [39]. Part of the difficulty in treating the polymer theoretically is the fact that multireference correlation increases as a conjugated π-bond network gets longer, and consequently the relative proportion of static and dynamic correlation captured by a given method will have a large effect on the BLA predicted for larger chains.

The BLA obtained from p2-RDM of the central bond of PA chains is plotted in Fig. 5.1,

along with the results from a number of other methods. As has typically been seen with p2-RDM, the results most closely resemble those of CCSD(T). CCSD and MP2 both fall substantially outside the experimental range, while Monte Carlo predicts a BLA in reasonably close agreement to experiment. The extrapolation used in Fig. 5.1 is of the form $Ae^{-BN} + C$. A recent work [35] examined various extrapolation schemes: the exponential fit, Kuhn's fit [40] ($A\sqrt{1 + 2B\cos\left(\frac{\pi}{1+N}\right)}$), and a linear combination of the two that would have 4 parameters. They concluded that the 4 parameter function gave the best fit for the data, particularly in the case of Monte Carlo. While both the exponential fit (0.080 Å) and Kuhn's fit (0.076 Å) gave reasonable values of the BLA for p2-RDM in the infinite limit, the 4 parameter function yields an unphysical prediction of 0.071 Å. However, given that the BLA from most methods is nearly converged by $N = 10$ or $N = 12$, it seems unlikely that the BLA of p2-RDM would drop an additional 0.011 Å in the infinite limit, and for that reason the 4 parameter fit is rejected for these data. It is also worth noting that the gap in BLA between p2-RDM and CCSD(T) widens as the chain lengthens. This is broadly consistent with past results, which have demonstrated that CCSD(T) captures more dynamic correlation than p2-RDM, while the latter captures more static correlation. It is unsurprising, therefore, that we see greater differences between the two methods for longer chains, for which multireference correlation is larger. When the BLA is shorter, single and double bonds are closer in length, allowing more configurations to contribute to the wavefunction; it seems that p2-RDM, with its greater tolerance of static correlation, is able to leverage that fact in order to lower the energy.

5.4 Discussion and Conclusion

In this work, we have for the first time implemented completely analytical nuclear gradients for the parametric two-electron reduced-density-matrix method. The p2-RDM method scales as $n^2h^4 + n^4h^2$, where n is the number of particles and h is the number of holes, and therefore, the single-point p2-RDM calculation is by far the most computationally expensive

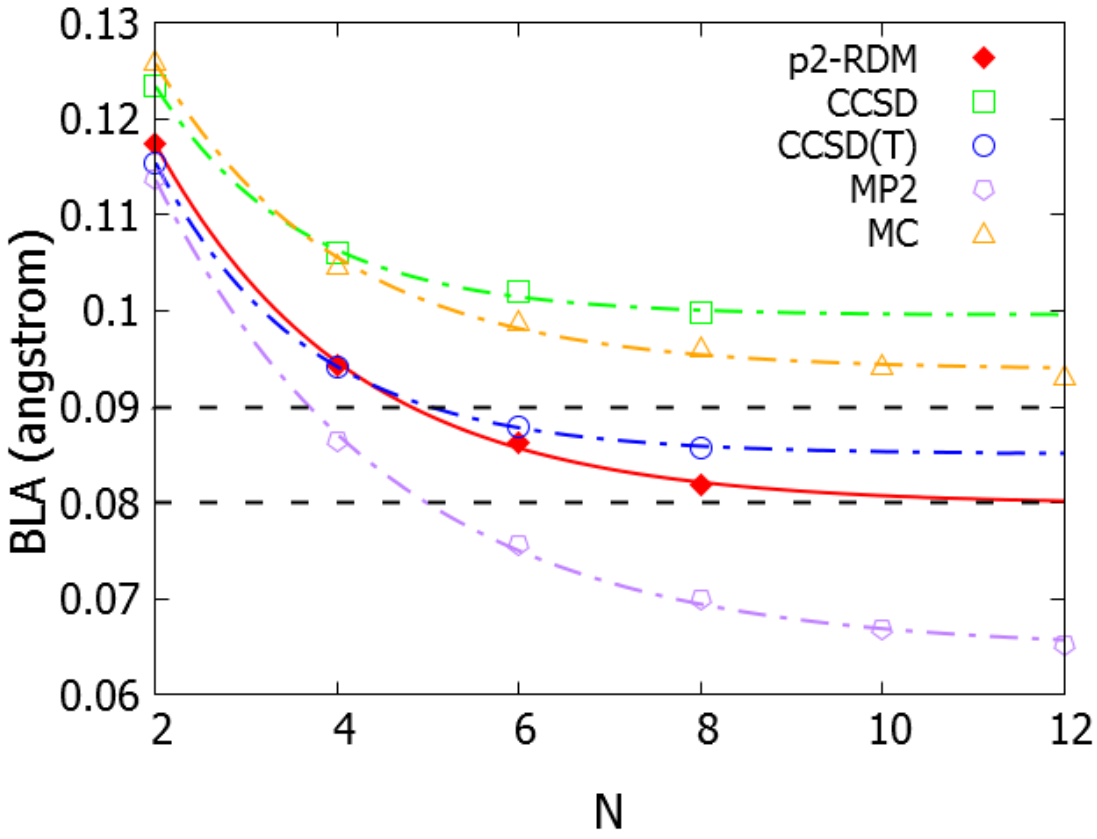

Figure 5.1: Bond length alternation (BLA) for *trans*-polyacetylene from various methods as a function of polymer length. Values are presented from p2-RDM, perturbation theory [38], Monte Carlo [35], and coupled cluster methods [39]. The upper and lower black lines are experimental values from NMR [36] and X-ray diffraction [37], respectively. Extrapolations of the data are of the form $Ae^{-BN} + C$. The parametric 2-RDM method predicts BLAs that are similar to those of CCSD(T), though closer to the experimental lower bound.

portion of the calculation. By limiting the number of single-point calculations required, analytical gradients dramatically decrease the computational cost of geometry optimizations. Even the small molecules used as benchmarks in this study saw sharp decreases in CPU times; for molecules with more nuclear degrees of freedom, the computational savings will be larger still. For example, the $N = 6$ *trans*-polyacetylene chain featured above would have computationally intractable using numerical gradients, and the $N = 8$ chain would have been unthinkable. Analytical nuclear gradients will allow us to apply p2-RDM's uniquely accurate and balanced treatment of strong electron correlation to systems of a size that were not previously accessible.

5.5 References

[1] A. J. Coleman and V. I. Yukalov, *Reduced Density Matrices: Coulson's Challenge* (Springer-Verlag, New York, 2000).

[2] A. J. Coleman, Rev. Mod. Phys. **35**, 668 (1963).

[3] F. Colmenero, C. Pérez del Valle, and C. Valdemoro, Phys. Rev. A **47**, 971 (1993).

[4] H. Nakatsuji and K. Yasuda, Phys. Rev. Lett. **76**, 1039 (1996).

[5] D. A. Mazziotti, Phys. Rev. A **57**, 4219 (1998).

[6] D. A. Mazziotti, Phys. Rev. Lett. **97**, 143002 (2006).

[7] R. Erdahl and B. Jin, *On Calculating Approximate and Exact Density Matrices* (Springer US, Boston, MA, 2000), pp. 57–84.

[8] D. A. Mazziotti, Phys. Rev. Lett. **106**, 083001 (2011).

[9] D. A. Mazziotti, Chem. Rev. **112**, 244 (2012).

[10] D. A. Mazziotti, Phys. Rev. Lett. **101**, 253002 (2008).

[11] A. E. DePrince III and D. A. Mazziotti, Phys. Rev. A **76**, 042501 (2007).

[12] C. Kollmar, J. Chem. Phys. **125**, 084108 (2006).

[13] C. A. Schwerdtfeger, A. E. DePrince III, and D. A. Mazziotti, J. Chem. Phys. **134**, 174102 (2011).

[14] A. J. S. Valentine and D. A. Mazziotti, J. Phys. Chem. A **117**, 9746 (2013).

[15] A. E. DePrince III, E. Kamarchik, and D. A. Mazziotti, J. Chem. Phys. **128**, 234103 (2008).

[16] A. M. Sand, C. A. Schwerdtfeger, and D. A. Mazziotti, J. Chem. Phys. **136**, 034112 (2012).

[17] P. Pulay, Mol. Phys. **17**, 197 (1969).

[18] A. C. Scheiner, G. E. Scuseria, J. E. Rice, T. J. Lee, and H. F. Schaefer III, J. Chem. Phys. **87**, 5361 (1987).

[19] J. E. Rice, R. D. Amos, N. C. Handy, T. J. Lee, and H. F. Schaefer III, J. Chem. Phys. **85**, 963 (1986).

[20] A. Brces, R. M. Dickson, L. Fan, H. Jacobsen, D. Swerhone, and T. Ziegler, Comput. Phys. Commun. **100**, 247 (1997).

[21] W. Hu and G. K.-L. Chan, J. Chem. Theory Comput. **11**, 3000 (2015).

[22] A. E. DePrince III and D. A. Mazziotti, J. Chem. Phys. **130**, 164109 (2009).

[23] A. E. DePrince III and D. A. Mazziotti, J. Chem. Phys. **133**, 034112 (2010).

[24] E. P. Hoy, C. A. Schwerdtfeger, and D. A. Mazziotti, Mol. Phys. **110**, 765 (2012).

[25] D. A. Mazziotti, Phys. Rev. A **81**, 062515 (2010).

[26] F. Wennmohs and F. Neese, Chem. Phys. **343**, 217 (2008).

[27] R. Ahlrichs, Comput. Phys. Commun. **17**, 31 (1979).

[28] J. Gerratt and I. M. Mills, J. Chem. Phys. **49**, 1719 (1968).

[29] N. C. Handy and H. F. Schaefer III, J. Chem. Phys. **81**, 5031 (1984).

[30] Y. Yamaguchi, Y. Osamura, J. D. Goddard, and H. F. Schaefer III, J. Chem. Educ. **72**, A42 (1995).

[31] E. F. Valeev, *Libint: A library for the evaluation of molecular integrals of many-body operators over gaussian functions*, http://libint.valeyev.net/ (2017), version 2.3.1.

[32] D. C. Liu and J. Nocedal, Mathematical Programming **45**, 503 (1989).

[33] S. Bochkanov and V. Bystritsky, www.alglib.net (2013).

[34] R. A. Kendall, T. H. D. Jr., and R. J. Harrison, J. Chem. Phys. **96**, 6796 (1992).

[35] M. Barborini and L. Guidoni, J. Chem. Theory Comput. **11**, 4109 (2015).

[36] C. S. Yannoni and T. C. Clarke, Phys. Rev. Lett. **51**, 1191 (1983).

[37] Q. Zhu, J. E. Fischer, R. Zusok, and S. Roth, Solid State Commun. **83**, 179 (1992).

[38] D. Jacquemin, A. Femenias, H. Chermette, J.-M. André, and E. A. Perpète, J. Phys. Chem. A **109**, 5734 (2005).

[39] D. Jacquemin, E. A. Perpète, G. Scalmani, M. J. Frisch, R. Kobayashi, and C. Adamo, J. Chem. Phys. **126**, 144105 (2007).

[40] J. Gierschner, J. Cornil, and H.-J. Egelhaaf, Adv. Mater. **19**, 173 (2007).

CHAPTER 6

INCREASING THE STABILITY OF THE PARAMETRIC TWO-ELECTRON REDUCED-DENSITY-MATRIX METHOD: A NEW FUNCTIONAL

6.1 Introduction

The parametric two-electron reduced-density-matrix (2-RDM) method has proven to be an accurate electronic structure method with a desirable computational scaling. One of the most promising aspects of p2-RDM is its ability to detect substantial multireference correlation effects, as it is able to correct poor reference wavefunctions much more than comparable single reference methods. However, in certain cases where the system is particularly multireference and the reference wavefunction is exceptionally poor, p2-RDM may fail to converge. In this chapter, I will present a derivation of the method, and using it, I will highlight where and why this lack of convergence can occur. With this understanding, I will propose a new parameterization that may resolve the issue. Lastly, I will present calculations on the nitric oxide dimer $(NO)_2$, a very difficult system for single-reference methods such as p2-RDM to treat.

6.2 Derivation of Parametric 2-RDM methods

Configuration interaction with double excitations (CID) postulates the following wavefunction ansatz

$$|\Psi\rangle = T_0|\Phi_0\rangle + \sum_{\substack{i<j \\ a<b}} {}^2T_{ij}^{ab}|\Phi_{ij}^{ab}\rangle. \tag{6.1}$$

The wavefunction is comprised of the reference Slater determinant $|\Phi_0\rangle$ (often obtained from Hartree-Fock) and all possible determinants $\{|\Phi_{ij}^{ab}\rangle\}$ generated by exciting two electrons out of the occupied orbitals i and j into the virtual orbitals a and b. Orbitals that are occupied

in the reference determinant are denoted by the letters $\{i, j, k, l, m, n, o, p\}$, orbitals that are unoccupied are denoted by $\{a, b, c, d, e, f, g, h\}$, and arbitrary orbitals are designated as $\{p, q, r, s\}$. The goal of CID is to vary the weights ${}^2T_0$ and $\{{}^2T_{ij}^{ab}\}$ so as to minimize the electronic energy

$$E = \langle \Psi | H | \Psi \rangle. \tag{6.2}$$

This energy can be broken into two components: the reference energy E_0, equal to $\langle \Phi_0 | H | \Phi_0 \rangle$, and the correlation energy E_{corr}, defined as the difference between the total electronic energy in Eq. 6.2 and E_0. The correlation energy can be expanded as

$$\begin{aligned} E_{corr} &= \Delta E + V_0 + V_{ij} \\ &= \sum_{\substack{i<j \\ a<b}} ({}^2T_{ij}^{ab})^2 \Delta E_{ij}^{ab} + \sum_{\substack{i<j \\ a<b}} {}^2T_0 {}^2T_{ij}^{ab} {}^2V_{ij}^{ab} + \frac{1}{2} \sum_{\substack{i<j \\ a<b}} \sum_{\substack{k<l \\ c<d}} {}^2T_{ij}^{ab} {}^2T_{kl}^{cd} \langle \Phi_{ij}^{ab} | H | \Phi_{kl}^{cd} \rangle. \end{aligned} \tag{6.3}$$

Here ΔE_{ij}^{ab} is the difference between the energy of the determinant $|\Phi_{ij}^{ab}\rangle$, or $\langle \Phi_{ij}^{ab} | H | \Phi_{ij}^{ab} \rangle$, and the reference energy E_0. The two-electron integral ${}^2V_{ij}^{ab}$ is the coupling element between the determinant $|\Phi_{ij}^{ab}\rangle$ and the reference, and $\langle \Phi_{ij}^{ab} | H | \Phi_{kl}^{cd} \rangle$ is the coupling element between two excited determinants. The first two terms in Eq. 6.3 are usually the most important. If the reference wavefunction was obtained from Hartree-Fock, which is the method of finding of the lowest-energy determinant possible, then ΔE_{ij}^{ab} will be non-negative for all excited determinants, and the first term ΔE will strictly be positive. CID is able to lower the energy, however, by balancing this increase in energy with the coupling V_0 between excited determinants and the reference, which is negative.

The coefficients $\{{}^2T_{ij}^{ab}\}$ must be bounded in some fashion: the wavefunction is normalized, such that

$$T_0 = \sqrt{1 - \sum_{\substack{i<j \\ a<b}} ({}^2T_{ij}^{ab})^2}. \tag{6.4}$$

If any coefficient $\{{}^2T_{ij}^{ab}\}$ increases in magnitude, T_0 must decrease, reducing the coupling

available to the other excited determinants. In effect, the normalization condition provides a restoring force that prevents amplitudes from increasing indefinitely. This presents a way of understanding one of the fundamental flaws of CID (and in fact, of any truncated form of CI): it is not *size-consistent*. A method if size-consistent if it gives an energy for two non-interacting molecules that is equal to the sum of the respective energies of each molecule. CID cannot be size-consistent because an excitation in one molecule reduces T_0 for the other molecule, reducing the coupling of the second molecule and ultimately increasing the energy. It was observed by Kollmar [1] that size-consistency could be restored by replacing the global T_0 of Eq. 6.4 with a determinant-specific term

$$\begin{aligned} {}^2T_{0,ij}^{ab} &= \sqrt{{}^2F_{ij}^{ab}} \\ &= \sqrt{1 - \sum_{\substack{k<l \\ c<d}} f_{ijkl}^{abcd} ({}^2T_{kl}^{cd})^2} \end{aligned} \tag{6.5}$$

where f is called the *topological factor*. If f is equal to 1 in all cases, Eq. 6.5 is of course equal to Eq. 6.4, and minimization of the energy would again give the CID result. However, if f is zero whenever $\{i,j,a,b\} \cap \{k,l,c,d\} = 0$, for instance when comparing an amplitude ${}^2T_{mn}^{ef}$ on one molecule and another amplitude ${}^2T_{op}^{gh}$ on a second molecule, the method is size-consistent because excitations on one moiety will not affect excitations on another non-interacting moiety. The parameterization depends upon the choice of f for different classes of elements. Kollmar [1] derived the K functional from considerations of partial N-representability conditions on the two-particle, two-hole, and one-particle-one-hole matrices, while Mazziotti [2] arrived at a different functional M by imposing particle-hole symmetry on the derivation. Later, an entire class of functionals $\mathrm{F}(\alpha,\beta)$ were proposed [3], to which K and M both belong. The various functionals are given in Table 6.1. Whatever the functional, these methods are collectively called parametric two-electron reduced-density-matrix (2-RDM) methods because the wavefunction in Eq. 6.1 is typically first directly contracted onto a 2-RDM.

Table 6.1: Various functionals f_{ijkl}^{abcd}, defined for classes of n_o/n_v, where n_o is the number of orbitals shared between (i,j) and (k,l), and n_v is the number shared between (a,b) and (c,d).

	Topological factor f_{ijkl}^{abcd}								
Method	0/0	1/0	2/0	0/1	0/2	1/1	2/1	1/2	2/2
CID	1	1	1	1	1	1	1	1	1
CEPA(0)	0	0	0	0	0	0	0	0	0
K	0	1/2	1	1/2	1	3/4	1	1	1
M	0	0	1	0	1	1	1	1	1
F(α,β)	0	α	1	α	1	β	1	1	1

6.3 Challenges from Strongly Multireference Systems

The parametric 2-RDM method has been seen to provide accurate energies for difficult electronic structure cases such as bond-breaking [4–6], transition states [7, 8], and diradical systems [9, 10]. These are all systems for which a restricted Hartree-Fock reference is insufficient to describe the wavefunction, yet p2-RDM has proven remarkably adept at correcting the qualitatively poor reference and revealing the true multireference character of the system. For example, the restricted HF reference used in Chapter 4 cannot possibly describe the two unpaired electrons of the diradical isomers of olympicene, yet p2-RDM finds that these isomers have strong radical character, in contrast to CCSD which finds hardly any radical character at all. However, when the reference is exceptionally poor, p2-RDM may on occasion fail to converge. To see why, examine the determinant-specific normalization in Eq. 6.5. This term can obviously only be real if ${}^2F_{ij}^{ab} > 0$, but we have imposed no constraints upon ${}^2T$ to force ${}^2F$ to be strictly positive. For systems that are mostly single reference, or well described by a single Slater determinant, the ${}^2T$ amplitudes are modest in size and no ${}^2F$ approaches zero. In contrast, if the system becomes sufficiently multireference and the reference becomes sufficiently poor, ${}^2T$ amplitudes may become very large and some ${}^2F$ terms may fall below zero, immediately terminating the optimization because ${}^2T_{0,ij}^{ab}$ has become imaginary. The effect of the reference on the convergence of p2-RDM can be subtle, as the method may converge at one geometry for a problematic molecule, yet fail

to converge at a slightly perturbed geometry. For such molecules, geometry optimizations are very difficult, because they require sampling many geometric configurations in order to find the minimum-energy structure. If any one single-point calculation fails to converge, the entire search algorithm may fail. A mechanism for altering the parameterization in order to treat these difficult systems would be greatly desirable.

To explore why p2-RDM may fail to converge, consider a strongly multireference system in which the two determinants $|\Phi_{mn}^{ef}\rangle$ and $|\Phi_{op}^{gh}\rangle$, with ΔE_{mn}^{ef} and ΔE_{op}^{gh} both small and ${}^2V_{mn}^{ef}$ and ${}^2V_{op}^{gh}$ both large, possess the largest amplitudes in the system ${}^2T_{mn}^{ef}$ and ${}^2T_{op}^{gh}$, respectively. Because $\{m, n, e, f\}$ and $\{o, p, g, h\}$ are disjoint, neither amplitude appears in the other determinant's topological factor, nor does the Hamiltonian directly couple the two determinants (as it only couples determinants that differ by at most two spin orbitals). As a result, neither amplitude is directly affected by the other. Consider now a third determinant, $|\Phi_{mp}^{eh}\rangle$, with a large ΔE_{mp}^{eh} and a small ${}^2V_{mp}^{eh}$, whose amplitude ${}^2T_{mp}^{eh}$ is very small. This determinant shares two indices with each of the first two determinants, whose amplitudes are therefore included in ${}^2F_{mp}^{eh}$. During the p2-RDM optimization, ${}^2F_{mp}^{eh}$ is the first term to fall below zero. As ${}^2F_{mp}^{eh}$ approaches zero during the optimization, we would expect the following forces to diverge

$$\begin{aligned}
\frac{\partial}{\partial {}^2T_{mn}^{ef}} V_{0,mp}^{eh} &= \left({}^2T_{mp}^{eh}\, {}^2V_{mp}^{eh} \frac{1}{\sqrt{{}^2F_{mp}^{eh}}} \right) {}^2T_{mn}^{ef} \\
\frac{\partial}{\partial {}^2T_{op}^{gh}} V_{0,mp}^{eh} &= \left({}^2T_{mp}^{eh}\, {}^2V_{mp}^{eh} \frac{1}{\sqrt{{}^2F_{mp}^{eh}}} \right) {}^2T_{op}^{gh}
\end{aligned} \tag{6.6}$$

and restrain the growth of ${}^2T_{mn}^{ef}$ and ${}^2T_{op}^{gh}$. However, if the product $|{}^2V_{mp}^{eh}\, {}^2T_{mp}^{eh}|$ is less than, say, $\sim 10^{-8}$ (not an uncommon occurrence) as ${}^2F_{mp}^{eh}$ approached zero, ${}^2F_{mp}^{eh}$ would have to be be greater than zero but less than $\sim 10^{-16}$ in order for the forces in Eq. 6.6 to be of numerical relevance. Clearly, from a computational standpoint, this is too narrow a range to present a substantial constraint on the magnitude of ${}^2T$.

6.4 A New Functional

One solution to a lack of convergence would be to explicitly enforce constraints on ${}^2T$ such that ${}^2F^{ab}_{ij}$ is positive for all $\{i, j, a, b\}$. However, this would remove one of the most desirable qualities of the parametric 2-RDM method: as an unconstrained optimization, the method is substantially faster than other constrained 2-RDM methods such as the variational 2-RDM method [11]. In addition, ${}^2F^{ab}_{ij}$ represents the population of the reference state: if this quantity falls near zero, the method has clearly failed to capture the qualitative character of the system. A better approach would seek to alter the parameterization such that no ${}^2F$ nears zero at all.

Even though CID is inaccurate even for systems of modest size, it does not suffer from a lack of convergence because the topological factor f in Eq. 6.5 is 1 for all pairs (i, j, a, b) and (k, l, c, d), treating every amplitude identically. However, this normalization prevents the method from being size-consistent. Parametric 2-RDM methods greatly relax the normalization condition by setting f to zero for the majority of pairs in order to restore size consistency, yielding lower and more accurate energies, but sometimes the remaining implicit constraints are not strong enough to prevent the optimization from straying into unfeasible regions. It stands to reason, then, that there must be a point on the spectrum between CID and parametric 2-RDM methods where the optimization is well-behaved yet the energy is still reasonably low and approximately size-consistent.

It would be tempting to search for a topological factor within the general $\mathrm{F}(\alpha, \beta)$ family outlined in Table 6.1, but as the above example is meant to show, it is possible even for $\mathrm{F}(\alpha, \beta) = \mathrm{F}(1, 1)$ (where $f = 0$ only for totally disjoint pairs) to lead to convergence issues if a system is sufficiently ill described with a single reference. In that example, ${}^2F^{eh}_{mp}$ falls below zero because both ${}^2T^{ef}_{mn}$ and ${}^2T^{gh}_{op}$ are very large, but the method does not explicitly couple the two amplitudes. However, if f^{efgh}_{mnop} were set to 1, the two amplitudes would be coupled and their magnitudes would be more constrained, possibly preventing ${}^2F^{eh}_{mp}$ from falling below zero. This suggests that explicitly coupling more amplitudes by setting f to 1

for more sets of indices may increase the likelihood of convergence. To that end, we propose a new functional featuring a set P, containing a number of amplitudes $\{^2T\}$. The topological factor f_{ijkl}^{abcd} will be equal to 1 if (i,j,a,b) and (k,l,c,d) share at least two indices, as before, or if there is a $^2T_{mn}^{ef}$ contained in P such that (i,j,a,b) and (k,l,c,d) each share at least two indices with (m,n,e,f). As more amplitudes are added to P, more implicit constraints will be added to the optimization, rendering the method more stable. Eventually, if enough amplitudes were included in P, the method would again become equivalent to CID, offering a systematic way of moving along the spectrum from parametric 2-RDM to CID. Most importantly, for the vast majority of systems that p2-RDM can already treat accurately, this parameterization would yield the same solution as the M functional because the set P would be empty.

The question remains of how to select amplitudes to be included in P. One option would be to wait until a given $^2F_{ij}^{ab}$ falls below a threshold, add $^2T_{ij}^{ab}$ to P, and then restart the algorithm. This has the advantage of focusing on the largest amplitudes, but it has the disadvantage of requiring the algorithm to first fail before attempting a correction. This is problematic because it would be very difficult to compare calculations between two species: if the optimization is immediately successful for one species, it will have used a different functional than the second. Instead, we propose adding $^2T_{ij}^{ab}$ to P in order of smallest ΔE_{ij}^{ab}. Determinants with a smaller ΔE are usually associated with larger amplitudes because their energetic penalty is smaller, so this choice of addition is also likely to target the largest amplitudes. Additionally, because the set P can be selected prior to the optimization, it will be easier to compare calculations of different species by specifying that each calculation include the same number of amplitudes in P.

6.5 The Nitric Oxide Dimer

In order to demonstrate the effect of this new functional, we examine the NO dimer. The equilibrium structure of singlet $(NO)_2$ is a C_{2v}-symmetric structure with an unusually long N-

Table 6.2: Equilibrium N-N bond length of the $(NO)_2$ dimer. Parametric 2-RDM results were found using the code from Chapter 5, while CCSD and CR-CC(2,3) were calculated in GAMESS [16–18]. Results from CCSD(T) and 2R-AQCC come from Ref. [19], while those of MRMP2(18,14) are from Ref. [20]. The p2-RDM bond length closely mirrors that of CCSD(T), and is substantially more accurate than other single-reference coupled cluster methods.

Method	cc-pVDZ	aug-cc-pVDZ	cc-pVTZ	aug-cc-pVTZ
CCSD	1.984	1.938	1.898	1.811
CR-CC(2,3)	2.154	2.095	2.052	2.028
p2-RDM	2.326	2.203	2.193	2.046
CCSD(T)		2.227	2.164	2.100
2R-AQCC	2.421	2.314	2.314	2.219
MRMP2(18,14)	2.455	2.383	2.385	2.436

N bond of 2.24-2.33 Å [12–15]. This can be viewed as either a highly stretched covalent bond or a very short range non-covalent interaction between two radical species; either scenario presents formidable challenges for a single-reference method. The conventional parametric 2-RDM method fails to converge for this species in certain basis sets and at certain geometries, making the global optimization of this species difficult. In order to optimize the geometry, we use the method outlined in Chapter 5, with a P that includes only the lowest-energy doubly-excited determinant. Even though P contains a single amplitude, p2-RDM now converges at every geometry and basis sampled. The equilibrium N-N bond length from p2-RDM, along with those of the single-reference coupled cluster methods CCSD, CR-CC(2,3), and CCSD(T) and the multireference methods 2R-AQCC and MRMP2(18,14) are plotted in Table 6.2.

The NO dimer is a somewhat unique molecule in that single-reference methods such as p2-RDM and CCSD(T) give more accurate bond lengths in small bases. As the basis set increases in size and becomes more diffuse, the dimer is stabilized in energy at shorter separations and the equilibrium bond length lessens. It appears that truly multireference methods such as 2R-AQCC and MRMP2 are required to accurately treat the dimer in the complete basis limit. As Tobita *et al.* observe [19], the dication of the NO dimer would be isoelectronic to two N_2 molecules, with four nearly degenerate π^* orbitals into which the

two additional electrons could be placed to make the dimer neutral again. This leads to many low-lying determinants that contribute strongly to the wavefunction and renders the molecule very highly multireference. That the equilibrium distance predicted by CCSD is off by 20% attests to the very poor quality of the reference. A single-reference method may partially compensate for a qualitatively poor reference by including excitations of high order, or in the case of p2-RDM, by relaxing constraints on the wavefunction such as normalization in order to increase the magnitude of double excitations. In this instance, the molecule is sufficiently multireference as to make convergence difficult for p2-RDM, but by adding only a *single* determinant to P, the method converges smoothly throughout the investigation. Additionally, despite potentially "corrupting" the method by including a small number of unconnected terms in Eq. 6.5, p2-RDM continues to predict structures that are more accurate that the comparable CCSD and the more computationally expensive CR-CC(2,3). This suggests that convergence issues within p2-RDM may be resolved by minimally altering the parameterization, preserving its important advantages of low computational cost, approximate size consistency, and flexibility in treating strongly multireference systems.

6.6 Concluding Remarks

The parameterization presented in this chapter is far from the final word on the topic. The use of a set P to alter the topological factor f is clearly not the only possible solution to convergence issues for p2-RDM, and even then, it remains an open question what the most desirable scheme would be for deciding which amplitudes to include within P. However, this scheme does appear to have several attractive features. It does not add any explicit constraints to the optimization nor does it alter the polynomial scaling of the method, so it is computationally efficient. It can be used to smoothly vary from the M parameterization to CID, allowing one to assess the degree to which the parameterization has been altered. And the NO dimer example suggests that maybe only very minor tweaks to the parameterization are required for convergence to be obtained. Above all, this work indicates that other classes

and forms of parametric 2-RDM methods may yet be found.

The M parameterization of p2-RDM suffers convergence issues only when the reference is particularly poor: for the NO dimer, a restricted Hartree-Fock wavefunction simply cannot qualitatively describe two doublet molecules interacting at relatively long range. In other words, *garbage in, garbage out*. The next stage in the evolution of p2-RDM methods may well be the formation of an explicitly multireference formulation, replacing $|\Phi_0\rangle$ in Eq. 6.1 with a multireference wavefunction (such as from CASSCF) and creating a method analogous to multireference CISD. With a qualitatively accurate reference, and preserving the computationally efficient and accurate inclusion of dynamic correlation from p2-RDM, such a multireference p2-RDM method could push the accuracy and applicability of 2-RDM methods to a level heretofore unseen. In addition, such a method could offer the possibility of extending the p2-RDM method to the treatment of excited states. Parametric 2-RDM methods are currently ill-suited for finding excited states because, among other reasons, it is unclear what single determinant could serve as the reference $|\Phi_0\rangle$. If an excited reference from CASSCF were used as $|\Phi_0\rangle$, the single and double excitations from p2-RDM could be used to stabilize the excited state, producing potentially very accurate excited-state energies. The field of parametric 2-RDM remains verdant, with many promising avenues for future developments.

6.7 References

[1] C. Kollmar, J. Chem. Phys. **125**, 084108 (2006).

[2] D. A. Mazziotti, Phys. Rev. Lett. **101**, 253002 (2008).

[3] D. A. Mazziotti, Phys. Rev. A **81**, 062515 (2010).

[4] A. E. DePrince III, E. Kamarchik, and D. A. Mazziotti, J. Chem. Phys. **128**, 234103 (2008).

[5] A. E. DePrince III and D. A. Mazziotti, J. Chem. Phys. **130**, 164109 (2009).

[6] C. A. Schwerdtfeger, A. E. DePrince III, and D. A. Mazziotti, J. Chem. Phys. **134**, 174102 (2011).

[7] A. M. Sand, C. A. Schwerdtfeger, and D. A. Mazziotti, J. Chem. Phys. **136**, 034112 (2012).

[8] A. E. DePrince III and D. A. Mazziotti, J. Chem. Phys. **133**, 034112 (2010).

[9] A. J. S. Valentine and D. A. Mazziotti, J. Phys. Chem. A **117**, 9746 (2013).

[10] A. L. McManus, E. P. Hoy, and D. A. Mazziotti, Phys. Chem. Chem. Phys. **17**, 12521 (2015).

[11] D. A. Mazziotti, Phys. Rev. Lett. **106**, 083001 (2011).

[12] C. M. Western, P. R. Langridge-Smith, B. J. Howard, and S. E. Novick, Mol. Phys. **44**, 145 (1981).

[13] S. G. Kukolich, J. Am. Chem. Soc. **104**, 4715 (1982).

[14] A. McKellar, J. Watson, and B. Howard, Mol. Phys. **86**, 273 (1995).

[15] S. G. Kukolich, Mol. Phys. **89**, 1659 (1996).

[16] P. Piecuch, S. A. Kucharski, K. Kowalski, and M. Musial, Comput. Phys. Commun. **149**, 71 (2002).

[17] P. Piecuch and M. Wloch, J. Chem. Phys. **123**, 224105 (2005).

[18] M. W. Schmidt, K. K. Baldridge, J. A. Boatz, S. T. Elbert, M. S. Gordon, J. H. Jensen, S. Koseki, N. Matsunaga, K. A. Nguyen, S. Su, T. L. Windus, M. Dupuis, and J. A. Montgomery, J. Comput. Chem. **14**, 1347 (1993).

[19] M. Tobita, S. A. Perera, M. Musial, R. J. Bartlett, M. Nooijen, and J. S. Lee, J. Chem. Phys. **119**, 10713 (2003).

[20] J. Ivanic, M. W. Schmidt, and B. Luke, J. Chem. Phys. **137**, 214316 (2012).